NOVEL COMPARATIVE STUDY AND CHARACTERIZATION OF PLANT DYES IN TiO_2 MATRIX FOR DYE SENSITIZED SOLAR CELLS APPLICATIONS

WANYONYI NAFUNA ELIZABETH (B.Ed SCI.)

I56/CE/24489/2012

A thesis submitted in partial fulfillment of the requirements for the award of the degree of Master of Science (Material Science) in the School of Pure and Applied Sciences of Kenyatta University

NOVEMBER, 2019

DECLARATION

This thesis is my original work and has not been presented for the award of a degree or any other award in any University.

Signature: ..... Date: 14/11/2019

Nafuna Elizabeth Wanyonyi

I56/CE/24489/2012

This thesis has been submitted for examination with our Approval as University supervisors.

Signature: ..... Date: 14.11.2019

Dr. Mathew Munji

Department of Physics

Kenyatta University

Signature: ..... Date: 14/11/2019

Prof. Justus Simiyu

Department of Physics

Massai Mara University

Signature: ..... Date: 14TH NOV 2019

Dr. Eric Masika

Department of Chemistry

Kenyatta University.

DEDICATION

This thesis is dedicated to my family members and my friends who encouraged me during the study.

ACKNOWLEDGEMENTS

I would like to take this opportunity to convey my sincere gratitude to my supervisors Dr. Mathew Munji (Kenyatta University), Dr. Justus Simiyu (University of Nairobi) and Dr. Eric Masika (Kenyatta University) for their commitment during this work.

I would like to thank all the members of the Department of Physics, Kenyatta University led by Dr. N. Hashim for the support and guidance during the departmental seminars.

I acknowledge the Vice Chancellor of Kenyatta University, Prof. P. Wainaina for providing conducive learning environment and unlimited internet for timely information access beneficial to this work. Technical staff members are sincerely thanked, special acknowledgement especially to the Chief Technologist Mr. F. Mudimba, who was always there for me for technical assistance. He availed all required apparatus and consumables, sometimes undertaking to be present beyond the call of duty. Many thanks go to the senior technologist solid state laboratories, University of Nairobi, Mr. B. Muthoka for his technical support during the optical measurements of the samples.

I wish to acknowledge my family members for their moral support and financial support throughout my studies. Above all, thanks to God for everything.

TABLE OF CONTENTS

DECLARATION .....**Error! Bookmark not defined.**
DEDICATION ii
ACKNOWLEDGEMENT iv
TABLE OF CONTENTS v
LIST OF TABLES viii
LIST OF FIGURES ix
ABBREVIATIONS AND ACRONYMS xi
ABSTRACT
CHAPTER 1
INTRODUCTION
1.1 Background to study 1
1.2 Statement of research problem 5
1.3 Objectives. 5
1.3.1Main objective 5
1.3.2. Specific Objectives 5
1.4Justification of the study 6
CHAPTER 2
LITERATURE REVIEW
2.1 Account of nano-crystalline dye sensitized solar cells 7
2.2 Related Studies……8
CHAPTER 3
THEORITICAL BACKGROUND
3.1Solar Cell Technology. 13
3.2 Dye Sensitized Solar Cells. 14
3.3 Components of DSSC 15
3.3.1 Fluorine doped Tin Oxide glass substrate 16
3.3.2 Photo- anode electrode. 17
3.3.3 Titanium dioxide 18

3.3.4 Counter- Electrode. 19
3.3.5 Dye sensitizer 19
3.3.6 Electrolyte. 22
3.4 The Philosophies of Dye Sensitized Solar Cells 23
3.4.1The operation principle of a DSSC. 23
3.4.2 Likely differences inside dye sensitized solar cells. 26
3.4.3 Photo-voltage and Photocurrent. 27
3.5 The Screen Printing Deposition Technique of the Photo-electrode. 29
3.6 Counter-Electrode Coat. 30
3.7 Solar Cell Parameters. 31
3.7.1 Solar Cell I-V Characterization. 31
3.7.2 Short circuit current *(I_{sc})* 31
3.7.3 Open Circuit Voltage (V_{oc}) 32
3.7.4 Maximum Power (P_{max}) 32
3.7.5 Fill Factor. 33
3.7.6 Efficiency (*I]*) 34
3.8 Optical Description 35
3.8.1 Optical reflectance 35
3.8.2 Optical Transmission. 36
3.8.3 Absorption of Light. 36
CHAPTER 4
MATERIALS AND METHODS
4.1 Introduction 38
4.2 Cleaning of substrates 38
4.4 Deposition of photo-electrodeand counter-electrode coatings 39
4.4.1 Screen printing on the photo-electrode 39
4.4.2 Graphite coating on the counter-electrode. 40
4.5 Annealing and sintering of the deposited layers 40
4.6 Sensitization of TiO_2 substrates. 40
4.7 Optical characterization 41

4.8 Cell Assembly 41
4.9 I-V characterization of the DSSCs 42
4.9.1 Diode characteristics. 42
CHAPTER 5
RESULTS AND DISCUSSION
5.1. Introduction 43
5.2 Optical characterization of FTO thin films.Figure 5.1Transmission Characteristics of single dyes. 44
5.3 I-V characterization of DSSC 55
5.3.1 Dark I-V characteristics. 55
CHAPTER 6
CONCLUSIONS AND RECOMMENDATIONS
6.1: Conclusion 68
6.2: Recommendations and further research. 69

LIST OF TABLES

Table 5.1: Transmittance of single dyes……..……...……44
Table 5.2: Transmittance of F.m and its mixtures……...……45
Table 5.3: Transmittance of Carrot and its mixtures……...……....47
Table 5.4: Transmittance of Orange and its mixtures…….48
Table 5.5: Comparison of the transmittance of mixed dyes and RU…….....49
Table 5.6: Reflectance characteristic of the single dyes. 51
Table 5.7: Absorption characteristics of single dyes**.** ……53
Table 5.8: Absorption characteristics of mixtures……....……..55
Table 5.9: I-V characteristic of single dyes…….55
Table 5.10: I-V summary for French marigold and its mixtures.……59
Table 5.11: I-V summary of Carrot and its mixtures……..58
Table 5.12: I-V summary of Orange and its mixtures……60
Table 5.13: I-V summary of dye mixtures……..61
Table 5.14: shows the summary of all the dyes used and their I-V characteristics..... 66

LIST OF FIGURES

Figure 1.1 Compacted state device representation diagram of a silicon solar cell(Anderson, *et. al*, 2007)..... 3
Figure 1.2 Schematic diagram of nano-particle-based dye sensitized solar cell (Ngogi *et al*., 2012..... 4
Figure 3.1Components of dye sensitized solar cell (Kay and Gratzel 1996). 16
Figure 3.2:Crystal structure of Titanium Dioxide (Kay and Grätzel, 1996) 18
Figure 3.3:Anthocyanin Molecule(Kay and Gratzel, 1996)..... 20
Figure 3.4: Molecular structure of the Anthocyanin molecule (Dadvar *et al*, 2012)..... 21
Figure 3.5:Molecular structures of carotenes and xanthophylls molecule (Dadvar *et al*,2012) 22
Figure 3.6: Operation principle of dye sensitized solar cell (Atalla, 2016) 24
Figure 3.7:Schematic Diagram of Energy Levels in components of DSSC (Shakir *et al*., 2017)…….26
Figure3.8: Electron injection recombination (Saleh *et al*., 2010) 29
Figure 3.9: Maximum power of I-V sweep (Sahnoun *et al*., 2015). 33
Figure 3.10: Fill factor from the I-V Sweep (Shakir *et al*., 2017) 34
Figure 5.1; Transmission characteristics of single dyes……..44
Figure 5.2: Transmission characteristics of French marigold and its mixture. 46
Figure 5.3: Transmission characteristics of carrot dye and its dye mixtures……...47
Figure 5.4:Transmission characteristic of Orange and its mixtures…….48
Figure 5.5:Transmission Characteristics of the dye mixtures…….…49
Figure 5.6: Reflectance characteristic of the single dyes.....51
Figure 5.7: Absorption characteristics of single dyed thin films…….52
Figure 5.8: Absorption characteristics of mixtures. 55
Figure 5.9:I-V Characteristics of DSSC of single dyes..... 57
Figure 5.10: I-V characteristics of DSSC of French Marigold dye and its mixtures…..…58
Figure 5.11: I-V characteristics of DSSC. Of carrot and its mixtures…….60
Figure 5.12: I-V characteristics of DSSC of Orange and its mixtures……..... 61

Figure 5.13: I-V Characteristics of DSSC of the dye mixtures…….... 63
Figure 5.14: I-V Characteristics of Ruthenium dye …….65

ABBREVIATIONS AND ACRONYMS

DSSC	Dye-sensitized Solar Cell
FF	Fill Factor
FTO	Fluorine Tin Dioxide
HOMO	Highest Occupied Molecular Orbital
InGaAs	Indium Gallium Arsenide
Io	Incident Photon
IR	Infra-red
Isc	Short circuit current
It	Intensity of Photon
I-V	Current and Voltage
L	Film Thickness
LUMO	Lowest Unoccupied Molecular Orbital
-OH	Hydroxyl Bonds
P max	Maximum Power
TCO	Transparent Conductive Oxide
TiO_2	Titanium Dioxide
TW	Terawatts
UV	Ultra-violet
Voc	Open Circuit Voltage
Hυ	Photon Energy
ɳ	Efficiency
α	Absorption Coefficient

ABSTRACT

A good energy mix is desirable for sustainability of the energy needs of many countries. Currently, electricity, including that sourced from photovoltaic cells is widely used for not only homesteads but also for industries. The desire to develop a cost-effective source of energy has motivated the development of dye sensitized solar cells. This technology has motivated a lot of research owing to its improved efficiency. This work has utilized plant extracts using a binder to develop a solar cell from locally available materials. Sieved extracts were obtained from carrot tubers, orange fruits and French marigold leaves. The juices extracted from each plant were stored in individual containers ready for sensitization. Ruthenium inorganic binder was used as a control. Screen printing technique was used to deposit titanium dioxide paste on the fluorine doped tin oxide glass slides. The developed thin films were annealed at a temperature of 450^{o}C in a furnace after which they were removed and allowed to cool ready for optical and electrical characterization. Using a DUV 3700 spectrophotometer, optical transmittance peak results indicated that ruthenium dye was transmitting at a peak of 47%, orange dye was transmitting at a peak of 30%, and French marigold dye was transmitting at a peak of 11% while the carrot dye was transmitting at a peak of 8%. On mixing different combinations of dyes in the ratio 1:1 by volume, the optical transmittance peak results indicated that the combination of carrot dye and French marigold dye was transmitting at peak of 27%, carrot dye and orange dye was transmitting at peak of 40% while French marigold dye and orange dye was transmitting at peak of 42%. These were higher than the transmittance peak values for single dyes. This was attributed to surface interaction. For reflectance characterization, orange dye peak reflectance was 24%, carrot dye peak reflectance was 14% while French marigold dye peak reflectance was 8% and the control dye was 15%. For absorption characterization (still in the range using DUV), French marigold dye absorption peaked at 91%, carrot dye absorbed at a peak of 92%, orange dye absorbed at a peak of 85% while the ruthenium dye absorbed at a peak of 84%. Electrical characterization of the solar cell was based on open circuit Voltage (V_{oc}) which was 0.482V for carrot dye, 0.433V for orange dye, 0.469V for French marigold dye and 0.565V for ruthenium dye. Short circuit Current (I_{sc}) was 0.0092 mA for carrot dye, 0.0099 mA for French marigold dye, 0.010 mA for orange dye, and 0.195mA for Ruthenium dye. The fill factor was 69.0% for carrot dye, 69.35% for French marigold dye, 67.1% for Orange dye while ruthenium dye had 58.1%. The obtained efficiency showed that carrot dye had an efficiency of 0.10%, French marigold dye had 0.097%, and orange dye had 0.087% while the control dye had 1.032%. From the study it was concluded that of the organic dyes Carrot dye gave a better efficiency of 0.100% and the least efficiency by orange dye. Ruthenium dye had the best efficiency of 1.032%. This was attributed to its wide spectral absorption. In conclusion therefore, a dye made of carrots juice could be more reliable as it has a higher efficiency. We recommend the purification of carrot dye before use to improve its efficiency.

CHAPTER 1

INTRODUCTION

1.1 Background to study

In present life, Electricity consumption has more or less become one of the basic needs of human life. Energy consumption dates back to the olden days where firewood was the main source. In the recent past, most of the consumed energy is from electricity. Traditional sources of energy have become insufficient. Most industrial energy consumption is accounted for by fossil fuel such as oil and natural gas. Since the original sources of energy are on the verge of depletion, nations are now venturing into new sources of energy production. Among the promising energy sources that are clean and with minimal pollution to the environment is solar energy (Nogi *et al*.., 2012).

Research conducted in the year 2013 showed that energy consumption stood at 18 terawatts (TW) in the whole world. This energy consumption was however projected to shoot to around 22 terawatts in the year 2025 (Zweibel, 2013). However, this figure is likely to swell because of the increasing population.

While making these anticipations, environmentalists are also warning the world about global warming. In the production of this energy, hydrocarbons produce energy with a significant ratio contributing to the greenhouse effect. The chemical reactions resulting from burning of fossil fuels produces harmful gases that take decades to dissipate. The gases produced increase the earth's mean temperature which changes the earth's climatic conditions.

With the recent technology, solar energy can be transformed into two forms. Firstly, solar energy is converted thermally and secondly solar energy can be converted into electricity by solar cells through photo-voltaic means. Solar energy from thermal conversion is used in heating systems such as heaters and water boilers whereas photovoltaic converts light to electrical energy that can be used for lighting, heating, cooling, refrigeration and power electrical appliances.

Photo-voltaic conversion in principle is where solar energy is transformed into electrical energy. This transformation is made possible by energy in light being used to break the strong bonds between atoms and electrons. This breakdown leads to free electrons as in the case of silicon crystalline solar cell.

A solar cell comprises n-type and p-type semiconductor materials. Figure 1.1 shows the components of a silicon solar cell. When the light photon hits the semiconductor, electron-hole pairs are separated into free electrons and holes. These free holes and electrons, with the help of the electric field, flow in different directions away from the p-n junction into the load.

The major semiconductors used in photovoltaics include crystalline silicon, indium gallium arsenide (InGaAs), cadmium telluride and copper indium selenide (Shah *et al*., 2004). Because of the observed low cost in solar energy consumptions, researchers have taken it upon themselves to find out how they can maximize solar energy production. Among the semiconductors used in solar cells, crystalline semiconductors have greatly revolutionized the solar industry because of their single crystalline nature. The major setback of crystalline

semi-conductors is the process of extracting them in the laboratories which is involving and also expensive. Desire for technology advancement has resulted in an increased interest in solar industry in the past years. A more simplified form of solar cells (DSSCs) have recently come into the market. Even though DSSCs face the challenge of efficiency, it is still highly researched on as compared to silicon solar cells because cheap materials are used in their construction (Marek, 2013).

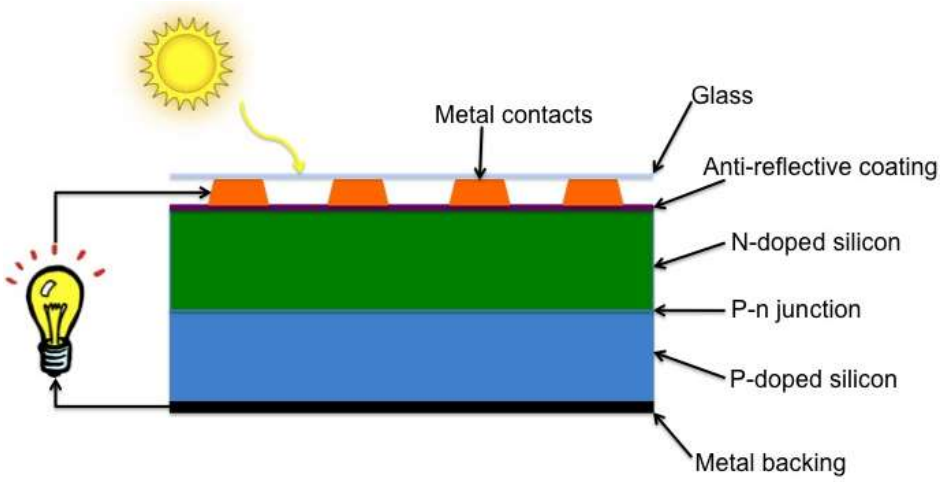

Figure 1.1: Schematic of a P-N junction solar cell (Anderson, *et. al*, 2007)

DSSCs employ dyes and electrodes glazed with a wide band gap semiconductor to hold the dyes used. The DSSC was launched in the early 1990s when non-crystalline TiO_2 was integrated with ruthenium bipyridl complex as dye sensitizer. These inventions were made by O'Regan and Grätzel (1991). They showed proof to the world in their project that DSSC solar cells were of low cost and higher efficiency because they employed organic materials in its structure (Travino, 2012). These DSSCs consist of an electrolyte sandwiched between conducting electrodes as indicated in figure 1.2

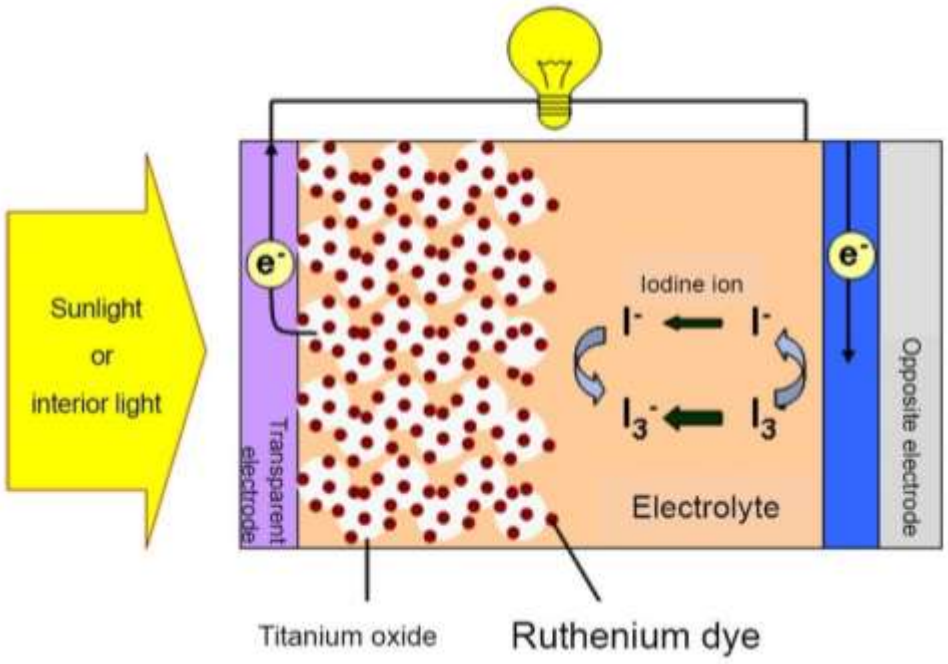

Figure 1.2: Schematic diagram of nano-particle-based dye sensitized solar cell (Ngogi *et al*., 2012)

A DSSC in principle has a transparent conductive oxide (TCO) coated glass substrate, a dye-sensitized nano-particle film, liquid electrolyte, and the counter electrode (Fig 1.2). The electrodes are made of transparent materials such that light photons can pass through into the cell. The dye is kept intact by the titanium dioxide that is anchored on the photo-anode. The principle function of the dye is to absorb light photons which excite electrons to cause current flow in the solar cell (McNelis *et al*, 1992). The function of the iodide electrolyte is to regenerate the electrons. The counter electrode however is made of carbon black, which ensures light does not pass through it (Likhtenshtein, 2012). The main content of this work was to develop a dye- sensitized solar cell from locally available dyes at low cost. The design involved the local materials such as orange juice, carrot tuber and French marigold. With these components, the device produced was quite efficient in energy conversion.

1.2 Statement of the research problem

The most popular dye that has been used in the past is ruthenium, which is relatively scarce in supply as it is obtained as a by-product from extraction of nickel and copper. It is expensive and poses environmental risk as it is mined. Research on alternative dyes that are organic, cheap and environmentally friendly has been ongoing. Plant dyes do not require a lot of processing and are obtained from gardens. When used on DSSC, they absorb light just like the process of photosynthesis. The absorbed photons aid in the conversion of solar energy to electrical power.

1.3 Objectives

1.3.1 General objective

To compare and characterize plant dyes in a TiO2 matrix towards solar energy conversion.

1.3.2. Specific Objectives

i. To extract the dyes from their natural plants using a blender
ii. To deposit dye sensitized Titanium dioxide paste on FTO glass substrates using screen printing technique.
iii. To study the optical characteristics of dye sensitized TiO_2 thin film coated on the FTO glass slides.
iv. To analyze and compare the I-V characteristics of the DSSC's prepared using different dye pigments.

1.4 Justification of the study

The working of DSSCs heavily relies on the type of the dye used. Ruthenium has a higher conversion efficiency than natural organic dyes. However, natural plant dyes are readily available, environmentally friendly, are cheap to prepare and absorb light in the visible range that is energetic enough to cause photo-excitation. The plant dyes adsorb efficiently on the semiconductors that aid in the electron percolation in the cell to produce electrical current.

CHAPTER 2

LITERATURE REVIEW

2.1 Account of nano-crystalline dye sensitized solar cells

Sensitization of semi-conductors to light of wavelength much higher than the conforming band gap was discussed in the history of DSSCs (Reddy, 2012). The principle of DSSCs operation depends on the convergence of photography and photo-electrochemistry. This two chemical practices depend on parting of liquid –solid interface (Reddy, 2012). TiO_2 is widely used in DSSCs because silver halides have band gaps of the order of about 3.0 which is insensitive to visible spectrum.

Vogel Berlin in the early 1870s studied allied dyes with halide semiconductors. This invention triggered more research in 1873 where panchromatic film rendered image of a scene realistically into black and white (Dadvar *et al.,* 2012). Few months later, the earliest sensitization of the photo-electrode was also invented with the same knowledge (Reddy, 2012). In principle, the two procedures of the DSSC can employ both dyes in both processes. The principle of action is just instillation of electrons from photo-excited dye molecules into the conduction band of n-type semiconductor substrates. As technology expanded in the subsequent years, it was noted that the dye functioned well if it was chemisorbed on the semi-conductor surface (Nogi *et al.,* 2012). This observation led to using dispersed molecules to give adequate interface in the presence of photo-electrodes.

Titanium dioxide was preferred for use for a number of reasons. Among the key reasons were: low cost, readily available, less toxic and biocompatible material. These factors are

important in sensitized photochemistry and photo-electrochemistry (Zhao, 2017). The dye that was widely used at the time was tris (2-2-bipyridyl-4-4 carboxylate) ruthenium (11). The main function of the carboxylate at that time was for the attachment by chemisorption of the chromophore to the semiconductor oxide substrate. Research on the DSSCs continued and in 1991, Gratzel announced electrochemical photovoltaic solar cell with the efficiency of conversion being 7 percent (Gratzel and O'Regan, 1991). The evolution then was explained by increased solar illumination, synergy structure, substrate morphology, dye photo physics and electrolyte redox chemistry. Latest developments show that the "black" dye (4, 9, 14tri-carboxy 2, 2'-6 6'- teryridly Ruthenium (11) tri-thiocyanate) was used at around late 1990s and the efficiency improved by at least one percent (Chou, 2011) Ruthenium bipyridyl complexes have transitional metals which are toxic and hard to synthesize. Because of this challenge, other natural sources of natural dyes have been discovered. Among the natural dyes discovered are rose Bengal, fluorescein and rhodamine B. These natural dyes, however have low performances as compared to ruthenium dyes (Labouret and Villoz 2012).

Improvements in the color sharpened sun-oriented cells have been very orderly. For example, panchromatic sensitizers have built up a solitary intersection photovoltaic cell that transfigures worldwide AM 1.47 daylight to power to retain light underneath 915nm wavelength at the limit. The carboxylate connections on the semi-conductor oxide surface ought to be firm so basic excitations infuses electrons into the strong with quantum yield of solidarity. These advancements in the panchromatic sensitizers have been intended to maintain around 108 turnover cycles which is assessed to be around 25 long stretches of

presentation to normal light. Color connections in the panchromatic sensitizers' guarantees unconstrained gathering as sub-atomic layer opens oxide layer to color arrangement (In Isoda, 2014).

In the field of organic dyes, quantum dot as sensitizers have also undergone a lot of transformations. Gratzel, 2006 said organic dyes are more used in DSSC fabrication than the inorganic dyes. Ruthenium complexes have also been widely used in this field and the efficiency has gone to about 11% (Gratzel, 2006). Hara *et al*. and the group have made improvements in the organic dyes for DSC in the past 3 years. Hara and the group used coumarine and polyene type sensitizers that achieved high sunlight to electric power conversion efficiencies of 8% in full sunlight. Latest developments have been identification of around 20 dyes which occur naturally. These dyes are obtained from flowers, plant leaves, fruits and indigenous beverages. These dyes contain cyanine, carotene and chlorophyll. In performance, photo-electrochemical properties of these dyes are Voc-0.559V and Jsc-2.50 $mAcm^{-2}$ (Zollinger, 2003).

2.2 Related studies

The principal utilization of color sharpened TiO_2 for sun-based vitality change was accounted for in a U.S. patent issued in 1978, in which a photographed electrochemical cell in view of color refinement of TiO_2 particles, especially in anatase shape (Chen, 2007). The color utilized was N-methyl-phenazinium particle which broadened the phantom reaction of TiO_2 to the 500-nm locale. In any case, the change proficiency of such a gadget was moderately low (around 4%) and the sunlight-based cell was shaky.

A vital advancement happened in 1991 when Gratzel and O'Regan announced a photo electrochemical sun powered cell utilizing nano-molecule TiO_2 sharpened by a more proficient and stable Ruthenium (11)- complex color. The standard color utilized in present cells is Ruthenium (11) (4,4'dicarboxy-2,2'- bipyridine)2$(NCS)_2$ with an ingestion crest at 550nm. This framework indicated transformation efficiencies of somewhere in the range of 7% and 10% under standard test conditions (STC). As of late, new "dark" color (4, 9, 14-tricarboxy 2, 2'- 6, 6'- terpyridyl Ruthenium (11) tri-thiocyanate) that delivered a proficiency of about 11% has been accounted for (Grätzel, 1997). Be that as it may, this sun-based cell was costly to manufacture as it required costly dyes.

The color sharpened sun-based cells are not quite the same as the run- off- the- mill silicon-based cells and have been classified into electro-compound cells and nano-crystalline cells (polymer-based sun-oriented cells and also color sharpened sun powered cells). The last are the focal point of this examination venture (Lynn, 2010). The significant downside in the innovation utilized in the produce of the multi-intersection sun-based cells is that it is costly and in this manner an option and less expensive technique is vital.

Kay and Grätzel (1996) beforehand utilized solid surfaces of single precious stone semiconductors as the electron conduction layer to which the color atoms were connected. This displayed an issue since the individual color particles retained under 1% of the approaching light. A better arrangement was than utilize colloidal coatings of nano-crystalline titanium dioxide (TiO_2). A nearby match vitality levels is required for the proficient infusion of photograph energized electrons from the color into the cathode and so far TiO_2 has all the earmarks of being the best choice. TiO_2 demonstrates a moderately little

conductivity in its unadulterated state (Grätzel, 2007). It is consequently that this oxide was utilized in this exploration venture.

Since the counter-anode decreases the oxidized electrolyte (tri-iodide to iodide) so they can again recharge the electrons lost by the color/sensitizer, it is critical for the counter cathode that it has a high electro-reactant movement to lessen the electrolyte (Hara and Arakawa, 2003). One of the components that have the best execution as a counter-cathode is platinum as it was utilized by Kroon *et al*.., (2007). Be that as it may, the staggering expense of this material and its constrained accessibility is an issue while considering minimal effort mass-produce of sunlight based (Snaith *et al*., 2007). A reasonable material that is both economical and has a decent reactant action is carbon which will be the material of decision utilized for this task as the counter terminal covering.

(Mawyin, 2009) announced that a standout amongst the most usually utilized sensitizers is mixes containing Ruthenium bipyridyl buildings. Nonetheless, these colors contain progress overwhelming metals that are dangerous and difficult to orchestrate and costly. As an option in contrast to Ruthenium colors, he proposed different wellsprings of natural sensitizers, for example, rose Bengal, fluorescein and rhodamine B, rosella and blue pea blossoms since these common colors, he announced, don't have the elite of Ruthenium colors yet their accessibility and relativity non-poisonous quality benefits proceed with research on their utilization with DSSCs.

Imahori *et al*, (2011) revealed that numerous sensitizers including inorganic and natural colors have been utilized in DSSC manufacture. Of the considerable number of sensitizers revealed the Ruthenium buildings were the most favored as a result of their high change

effectiveness which has come to 11% (Grätzel, 2006). Ruthenium complex colors were said to have higher costs. In any case, polypyridine edifices of Ruthenium have extraordinary charge exchange retention over the entire unmistakable range and have simple tune-capable redox properties making them gain a high ground on other metal sensitizers. In any case, natural colors have higher molar termination coefficients than Ruthenium complex colors thus are favored in creation of minimal effort DSSCs.

Zhou *et al*. (2015) got twenty colors acquired from nature, including blossoms, leaves of plants, organic products, customary Chinese pharmaceuticals and drinks. These colors were utilized as sensitizers in DSCs. The colors separated from these materials contained cyanine, carotene and chlorophyll. The photograph electrochemical execution of the DSCs in light of these colors demonstrated that the Voc ran from 0.337 to 0.689V and Jsc was in the scope of 0.14 to 2.69 mAcm−2. The DSC sharpened by mangosteen pericarp extricate offered the most astounding change proficiency of 1.17% among the 20 separates. In any case, blackberry and raspberry colors were not utilized in DSC manufacture.

CHAPTER 3

THEORETICAL BACKGROUND

A solar cell is an electrical device that converts light energy directly to electrical energy by photovoltaic effect through physical and chemical phenomena. It is a photoelectric cell whose electrical features, e.g. current and voltage depends on its exposure to sunlight. Solar cells are collectively called solar panels. In principle, solar cells are used for detecting electromagnetic radiation and measuring light intensity. The solar cell is a P-N junction that is made up of dyes or polymers.

3.1 Solar Cell Technology

The first ever solar cell was developed in 1839 by Edmond Becquerel (Alyssa, 2016). Becquerel noticed that electricity could be generated by a piece of silver chloride illuminated with sunlight. This conversion of sunlight to electricity was estimated to be around 1%, (Alyssa, 2016). Australian Andrew Blakers and Martin Green have made a significant effort in the manufacturing of over 30 percent of solar cells in the past 3 decades. Consequently, the solar cell manufacturing technology has since spread all over the world. The commonly used solar cells are made from wafers of ultra-pure (99.99%) silicon and boron that have been infused with phosphorous in the 2000^{o}c hot furnace, coated with antireflection material and fired with metal contacts. The solar cells have electric field at its heart that splits negative charges from positive charges using light energy. The electric field in the coating of the cell is set up with other atoms. The boron atoms are less on one side and phosphorous atoms more on the other side of the wafer. These atoms together create the P-N junction. In

electrostatics, opposite charges attract but due to the presence of the P-N junction, the electric field pushes positive and negative charges separate. The moment the solar cell absorbs sunlight, an electron is energized inside the silicon and is driven across the coating by the electric field. This electron is trapped at the metal contacts and is converted to usable electricity. Once the sunlight shines on solar panel, DC electricity is moved to conductors into the inverter that transforms DC to 240V AC supply used in homes.

As far as technology grows, the solar cell efficiency as at now stands at 40 percent on normal sunlight and 46% for intense light that is equal to 300 suns. However, the latter which involves focusing sunlight on a large area with a bunch of mirrors is used in space and is made of very expensive materials (Allen, 2017).

3.2 Dye Sensitized Solar Cells

Dye Sensitized solar cell is a relatively cheap thin film solar cell that is founded on semi-conductor made between photosynthesized anode and an electrolyte in a photochemical process. DSSC was invented in the late 1960s by Brian O'Regan and Michael Grätzel and later transformations by Ecole Polytechnique Federal de Lausanne who led to the first ever efficiency to be realized in 1991.

Research on the DSSC has intensified because of the following reasons: simply made by conventional roll-printing techniques, it is semi-transparent and semi flexible hence its many other uses and its use of low-cost materials in its construction. The main challenge to DSSC is the high cost of acquiring ruthenium and platinum materials and finding the electrolyte that is suitable in all weather conditions (Feihl., 2014). It was found out in the University of

California that illuminated organic dyes generated electricity at oxide electrodes in the electrochemical cells (Kalyanasundaram, 2010).

At the same university, chlorophyll was removed from spinach through the biometric system which was used to explain electric generation through the dye sensitization solar cell in the year 1972, (Kalyanasundaram, 2010). The challenge identified at that time was the instability of the dyes. Projections were made on how to improve the efficiency of the solar cell and it was suggested that boosting the porosity of the electrode made could solve the problem. In DSSC, titanium dioxide is used which is more porous and covered with molecular dye which absorbs light (Markart, 2000). Sunlight then penetrates the photo electrode into the dye exciting electrons which flows into the titanium dioxide. The electrons then flow and recollects at the photo electrode for powering the load. The electrons thereafter flow into the external circuit and are reintroduced into the cell on the counter electrode flowing into the electrolyte. Electrons are finally transmitted back by the electrolyte to the dye molecules (Kalyanasundaram, 2010).

3.3 Components of DSSC

The DSSCs discussed in this work are based on the principle laid down by Kay and Gratzel (1996). Fig 3.1 shows the main components of the DSSC which are: titanium dioxide which acts as the photo-electrode, carbon layer which acts as a counter-electrode, conductive glass substrate, organic dye sensitizer which is used for electrode sensitization and regeneration of electrolyte as the redox duo. In the whole process, iodide ions are the active ions in the electrolyte.

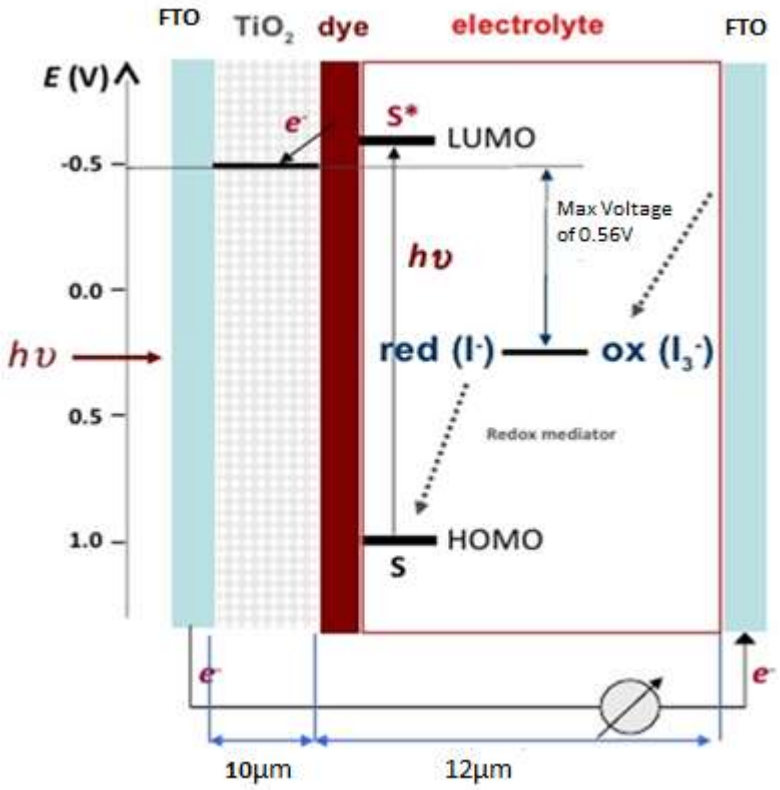

Figure 3.1: Components of dye sensitized solar cell (Kay and Gratzel 1996).

3.3.1 Fluorine doped Tin Oxide glass substrate

The DSSC substrates consist of either glass or plastic materials and are basic components. In most cases, glass substrate is used because it can withstand sintering temperatures close to 500^{o}C. The glass substrate is transparent to maximize the sunlight coming in and possess conducting properties so as to allow photo-generated electron not to flow in the hole direction.

The glass substrate is glazed with fluorine tin dioxide (FTO) which is stable at high temperatures. The other desirable properties of FTO are: good transmittances of about 83%

depending on the thickness, low resistivity of about $1.9*10^{-6}$Ωm and the ability to withstand high temperatures during annealing processes (Main, 2012).

3.3.2 Photo- anode electrode

In the DSSC, semi-conductor material is deposited on the photo-electrode. Photo-electrode is a conductive electrode which acts as the anode and is responsible for high porosity area where the dye sensitizer is anchored and ensures titanium dioxide acts as a layer where excited electrons are moved to from the dye sensitizer. The latter process happens suddenly to reduce recombination losses. In past technologies, solar experts employed monolithic surfaces of single crystal semi-conductors onto which dye molecules were anchored. This technology however suffered setbacks because the dye molecules absorbed less than 2 % of the sunlight (Dadvar *et al.*, 2012). This challenge triggered intense research and physicists found out that use of nano-crystalline titanium dioxide coatings gave a relatively high percentage. The new technology of using porous titanium dioxide increased the surface area in which the sensitizer could absorb more light energy for better results of the excited electron particles (Kay and Grätzel, 1996).

In past advances, sunlight-based specialists utilized solid surfaces of single precious stone semi-conductors onto which color particles were appended. This innovation however endured misfortunes in light of the fact that the color atoms consumed fewer than 2 % of the daylight (Dadvar *et al.*, 2012). This test activated extraordinary research and physicists discovered that utilization of nano-crystalline titanium dioxide coatings gave a moderately high rate of absorption. The new innovation of utilizing permeable titanium dioxide

expanded the overlap surface territory in which the sensitizer could assimilate more light for high aftereffects of the energized electron particles (Kay and Grätzel, 1996).

3.3.3 Titanium dioxide

It is a wide-band gap semi-conductor with the molecular formula TiO_2. It is non- toxic, most available compound in nature apart from sand. Titanium dioxide is the stable compound responsible for the bright white appearance in most materials such as paints.

The structure of titanium dioxide has both ionic and covalent bonds. These bond types guarantees TiO_2 to be insulating in its stoichiometric crystals. Figure 3.2 shows titanium dioxide's bonding structure in 3D.

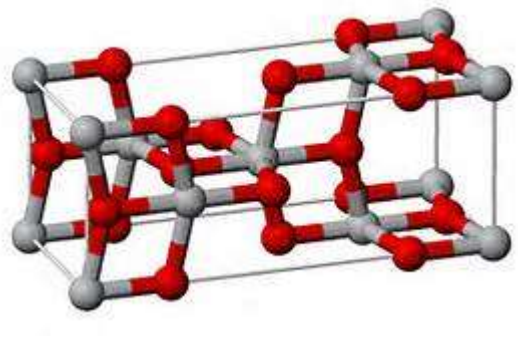

Figure 3.2: Crystal structure of titanium dioxide (Kay and Grätzel, 1996)

The red spherical balls are the oxide ions while the white spherical balls are titanium ions. The conduction bands in the titanium dioxide are matched to the excited energy levels of organic dyes in the case as that of the carotenes. This matching is vital in ensuring that photo-excited electrons are efficiently injected from the dye into the electrode. The small conductivity of the pure titanium dioxide is increased upon photo-generated electron injection. Increasing injection of the photo-generated electrons reduces the ohmic losses.

Recent technologies, however indicate that doping the titanium dioxide improves its performance (Stubhan et al.., 2012).

Titanium dioxide has three phases namely: rutile, anatase and brookite. Anatase phase is the commonly used phase in the solar industry because of its large energy band of 3.3eV. The anatase phase is used in the manufacture of the electrode which has annealed and sintered coating of nano-crystalline particles (Kay and Grätzel, 1996).

3.3.4 Counter- Electrode

Counter-electrode is responsible for reduction process in the electrolyte. The oxidized tri-iodide is reduced to iodide to replenish the lost electrons by the dye-sensitizer. Platinum element is preferred in the counter-electrode because of its high electro-catalytic activity to reduce the electrolyte **(**Kalyanasundaram, 2010). Carbon however is used on the counter electrode as it is cheap and easily available as compared to platinum. Carbon counter-electrode has been used in this work (Stubhan *et al*.., 2012). The carbon used in this research was obtained from an ordinary pencil. This carbon has good desirable characteristics despite being fragile and vulnerable to abrasion. Recent tests in the labs are embracing this carbon because of its availability and the low cost involved in acquiring it (Dadvar, *et al*, 2012).

3.3.5 Dye sensitizer

Dye sensitizers have hydroxyl (-OH) and carboxyl (-COOH) groups. These features enable the sensitizers to anchor themselves on the oxide of titanium. Electrons produced by the dye are moved through the molecule into the titania. The electrons on the titanium dioxide attached to the conductor can be harnessed for useful applications. The usefulness of these electrons can be witnessed by the power produced by the light bulb. Since the electrons

produced by the dye gets depleted, redox electrolyte is used to give back electrons to the dye. The electrolyte gets its electrons from the return of dye-regenerated electrons that were sent through the circuit. This process circumnavigates to ensure electrons are never depleted.

Dye sensitizer is naturally found in the orange fruit which is an example of anthocyanin molecule.

Figure 3.3: Anthocyanin molecule (Kay and Gratzel, 1996)

In DSSC, sensitizers are highly photo-sensitive. This desirable characteristic aids in the light absorption which has energy equal to the separation of low and high energy states in the dye and subsequent injection of electrons into the titanium dioxide. Electron injection process is more rapid to avoid photo-excited electrons to decaying back into the dye molecule. According to Seigo *et al*. 2006, the lifetime for injection and photo electron decay is in the range of femto-second and microsecond respectively. Seigo also argued that organic solar cell sensitizers can have absorption band personalized to a certain range. This argument is substantiated with solar cells that have multiple layers and dyes having a wide absorption

range which is used to absorb sunlight (Stubhan et al.., 2012). Below is a structure of anthocyanin molecule.

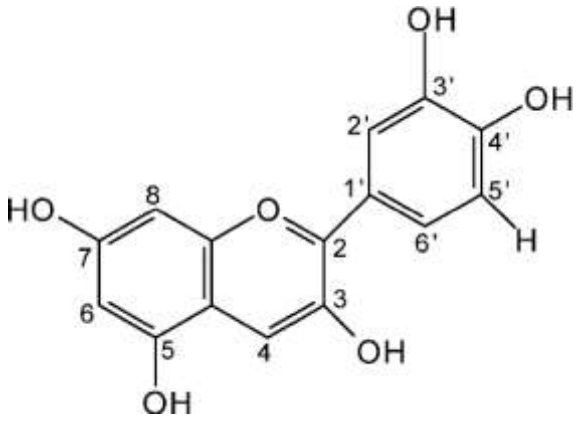

Figure 3.4: Molecular structure of the anthocyanin molecule (Dadvar *et al*, 2012)

The anthocyanin molecular structure has "=O" and the "- OH" sides which aid in the binding of dye molecule to the TiO_2 applied. The carotenes have carboxyl groups for the attachments to TiO_2

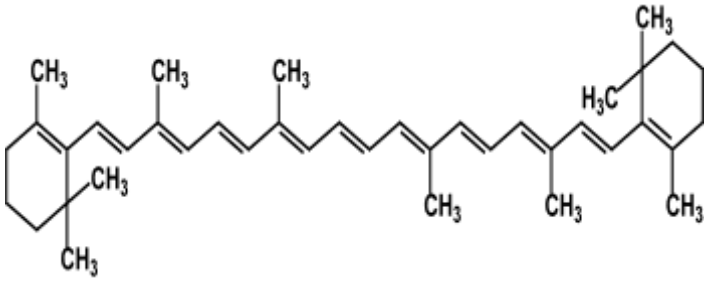

Figure 3.5 (a)

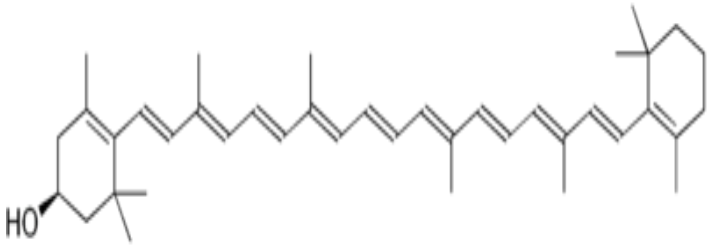

Figure 3.5 (b)

Figure 3.5: Molecular structure of carotene(a) and xanthophylls molecule(b) (Dadvar *et al*, 2012)

For xanthophylls, the hydroxide group ensures good bonding on the semiconductor. In the separation of the dye, we have HOMO and the LUMO levels. These two estimations are achieved through the following mathematical equations.

$$E_{HOMO\text{-}LUMO} = 1240/\lambda \quad (3.1)$$

λ represents the absorption peak in nanometers.

DSSC sensitizers are black in the UV, Visible and IR spectral region to maximize absorption of light. These DSSC also have energetic dynamic coupling between the photo-excited sensitizer and conduction band to ensure high efficiency in the light conversion. In principle, DSSC sensitizers have a strong photo-stability to prevent electron decomposition.

3.3.6 Electrolyte

DSSC electrolytes are ionic compounds having tri-iodide and iodine elements. Potassium iodide saturated with the iodine crystals is the most commonly used electrolyte in the DSSCs. This compound is widely used because it matches with the HOMO level of anthocyanin dye

(Kay and Grätzel, 1996). Apart from that, it also has a slow rate of reduction between the tri-iodide and the charges in the TiO_2 particles and hence reduced recombination losses (Kay and Grätzel, 1996). Chemical processes between charges and redox couple are rapid at the counter-electrode and less rapid at the photo-electrode so as to decrease the recombination losses (Stubhan et al.., 2012). The oxidation process is vital in replenishing iodide to tri-iodide solution by moving towards the counter-electrode through the reduction process.

$$I_2^- + 2e \longrightarrow 3I^- \qquad (3.2)$$

3.4 The Philosophies of Dye Sensitized Solar Cells

3.4.1 The operation principle of a DSSC

Grätzel and Greg, (1998) breaks down the operation principle of the dye sensitized solar cells as follows.

i. Incoming photon of light excites the electron in the dye monolayer.
ii. Electron injected into titanium dioxide.
iii. Electrons felt externally such as lighting a bulb.
iv. Reduction process at the counter-electrode.
v. Electron diffuses into the electrolyte.
vi. Oxidized dye regenerated back to the powdered state.

From the steps listed above, it is seen that electrons are excited in the dye monolayer in the first step. Most dyes used in the laboratories are about 700nm which is the range away from

the required dye parameters. Research on organic dyes have shown absorption window in VIS spectra (Stubhan et al.., 2012). Figure 3.6 shows the operation procedure of a DSSC.

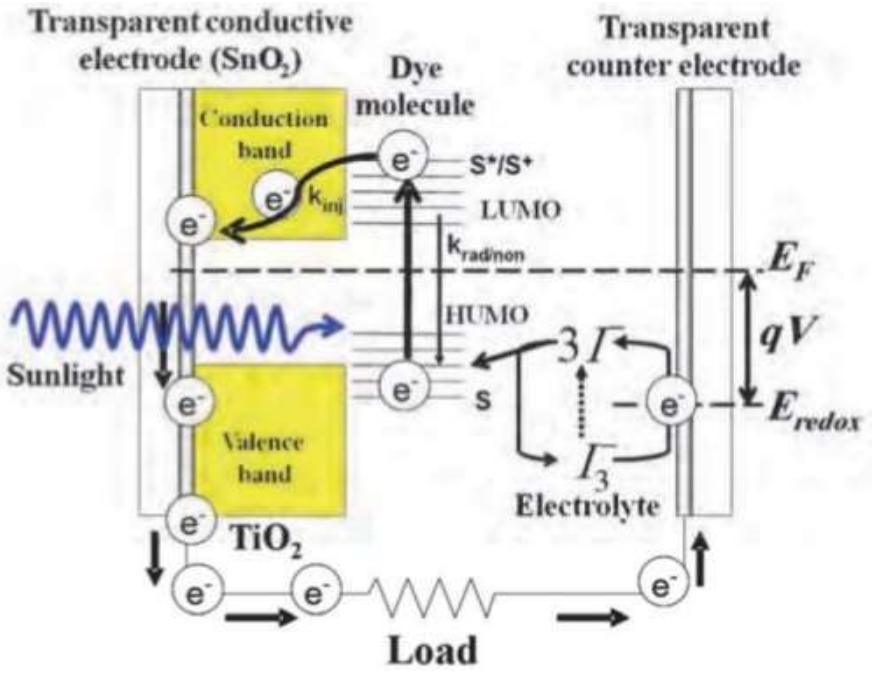

Figure 3.6: Operation principle of dye sensitized solar cell (Atalla, 2016)

After electron excitation, the second step is injection of the electron into the conduction band of the TiO_2 or any other semi-conductor. The process of electron injection occurs either in the singlet state or the triplet state. The singlet state is where injections are in femto-second range and the process occurs slower as compared to the triplet state (Regan *et al.*, 2005). It is advised that the energy level of the dye is above the TiO_2 conduction band edge to have maximum injection of the electrons. In the singlet state, the process is slower because we have low injection dynamic force and transfer chance. In principle, electron injection from the dye into the titanium dioxide occurs in a matter of pico-seconds while that of electron charge recombination occurs in a matter of milliseconds and microseconds. The chemical

back reaction process where the electron is moved to oxidized dye is required to be slow as compared to the reduction process of the oxidized dye to maximize charge injection. Since the reduction process is slower than the injection rate process, charge separation is possible in DSSCs (Zhang and Guozhong, 2011).

Systematically, the third step is achieved by electron going through the nano-porous TiO_2 layer. This layer is made of anatase particles which are about 25nm in length. The nano-porous layer has a weak n-doped structure due to the presence of oxygen openings in the trellis (Kumara *et al*., 2017). The conductivity of the flat band is high because surfaces are compared to the available surface is 1000 times higher and the thickness is about 9ϥmicrometers. Scientifically, the motion of electrons through the TiO_2 can be described by a model called de-trapping model (Kumara *et al.*, 2017). The movement of electrons depends solely on diffusion force. This means the diffusion lengths have to be more or less the same or more than that of the TiO_2.

The reduction process in the electrolyte is as a result of conduction band electrons. Step 4 explains iodine reduction process. After the electron has flown in the external circuit, it is moved to the electrolyte most likely tri-iodide solution. Tri-iodide solution however has a major shortcoming in efficiency hence new findings suggest sol-gel which has efficiency close to 5% (Wei *et al*., 2010) with a low short circuit current and constant open circuit voltage.

Carbon at the counter-electrode acts as a catalyst in the reduction process. Tri-iodide is used as an electrolyte in the DSSC although research is underway to find solutions to the corrosive

nature of the iodine to the metal contacts. Efficiency of the DSSC greatly depends on the reduction process at the counter electrode. It is discussed that iodine reduction at the counter electrode be faster as to the recombination process at the TiO_2 border in the electrolyte to achieve relatively higher efficiencies in the light conversion. In principle, regenerating oxidized dye back to the ground state occurs faster than recombination process and is believed to be 105 times faster than internal lifetime of the oxidized dye (Fara *et al.*, 2013).

3.4.2 Likely differences inside dye sensitized solar cells

For maximum efficiency in the DSSC, optimum match between relative energy levels of varied elements is important. As seen from figure 3.7, differences in relative locations of energy levels bring about a driving force for moving the charges.

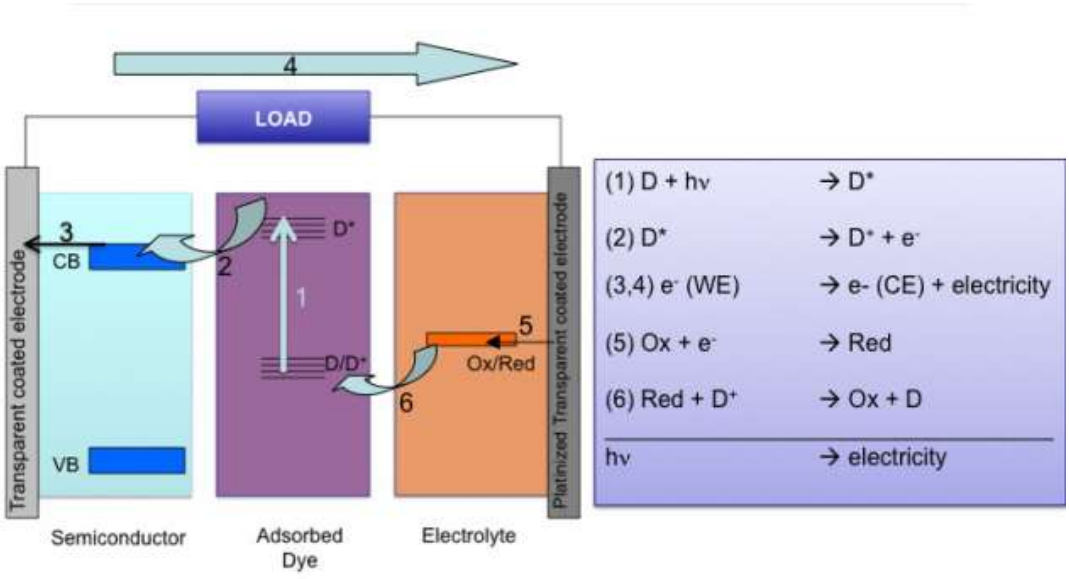

Figure 3.7: Schematic diagram of energy levels in components of DSSC (Shakir *et al*.,2017)

From Fig. 3.7 it can be seen that through the LUMO level, charges are moved to the conduction band by the injection process. From simple chemistry, the hole left after electron excitation is filled by electrons from the iodine ion reaction as shown in equation 3.3

$$3I^{-}+2h_{dye} \longrightarrow (3I)^{-}+dye^{o} \quad (3.3)$$

From, h_{dye} and dye^{0} is the oxidized dye^{0} and reduced dye respectively.

The counter electrode potential is estimated to be same as equilibrium potential of the redox process so as to get tri-iodide back to iodide. On the other hand, the potential level of the titanium dioxide is higher compared to potential electrolyte so that photoelectron recombination is reduced in the electrolyte (Wei *et al.,* 2010).

3.4.3 Photo-voltage and Photocurrent

The difference between the conduction band energy level of the TiO_2 and the redox potential level of the electrolyte brings about the photo-voltage in the DSSCs (Fara *et al*., 2013). Theoretically, maximum photo voltage can be calculated using energy levels and values of the intrinsic losses. In principle the intrinsic DSSCs losses are as a result of dye molecules losing holes to electrodes and recombination taking place with the injected electron before the collection process is done (Wei *et al*., 2010) and the voltage reductions occurring as a result of mismatch between energy levels of transparent coating oxide and mismatch between redox couple and the counter electrode. Latest developments in the DSSCs suggest careful selection of materials to be used in the DSSCs basing on their energy levels.

It is a fact that the generated photo current is directly proportional to charge injection rate of the photo-excited electrons from the HOMO level to the conduction band of the TiO_2 (Fara

et al., 2013). In summary, the electron path is from photo generation to injection and finally reduction. Solar energy experts say that recombination in the photocurrent is as a result of the following reasons:

Failure of the photoelectrons to be injected into the titanium dioxide but remaining in the LUMO level. This leads to the electron decaying to the ground state losing energy in the process. This event is however very rare because of the sudden electron injection into the $TiO_2$and slow recombination rate in the electrolyte.

The contrast between the conduction band level of the TiO_2 and the redox potential level of the electrolyte realizes the photograph voltage in the DSSCs (Moraru *et al*., 2013). Hypothetically, most extreme photograph voltage can be figured utilizing levels and estimations of the inborn misfortunes. On a basic level the natural DSSCs misfortunes are because of color particles losing gaps to cathodes and recombination occurring with the infused electron before the accumulation procedure is done (Wei *et al*., 2010) and the voltage reduction happening because of crisscross between levels of transparent coating oxide and jumble between redox couple and the counter terminal. Most recent improvements in the DSSCs recommend keen determination of materials to be utilized as a part of the DSSCs.

Secondly, in the event that electrons injected into TiO_2 recombine with the electrolyte when it is not yet collected at the back contact. Figure 3.8 shows the possible electron recombination paths.

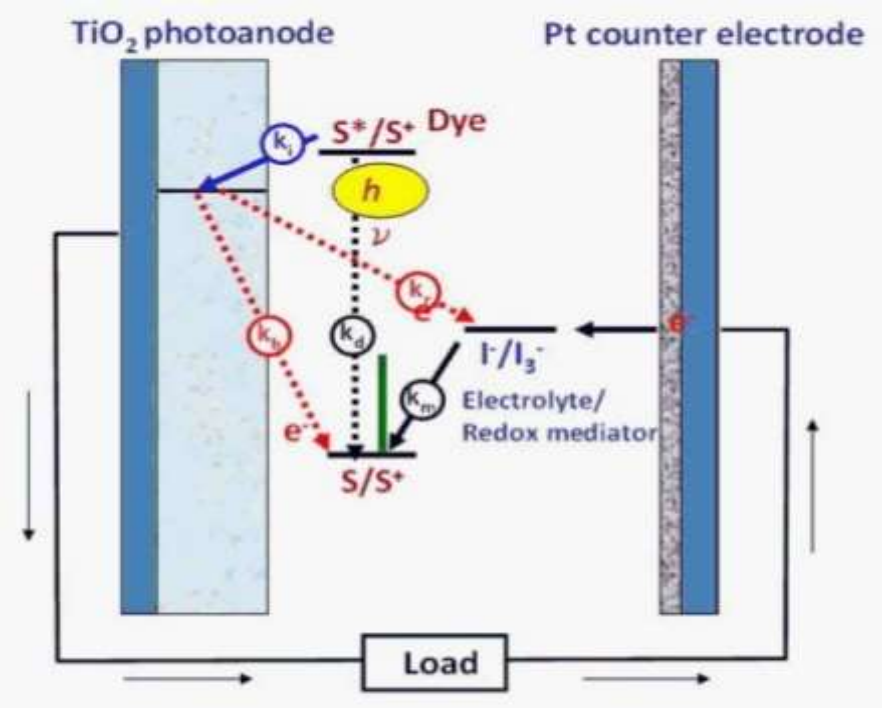

Figure3.8: Electron injection recombination (Saleh *et al*., 2010)

The above reaction is quite slow in the short circuit conditions and hence cause photo current also to reduce in value. On the other hand, in the event of the open circuit, the reaction causes the photogenerated carriers to be lost (Shakir *et al*., 2017). The above challenge can however be solved by increasing the surface area of the TiO_2 particles in contact with the absorbed dye molecules so as to buffer injected electrons from the electrolyte increasing light absorption capability of the dye (Bube, 1998).

3.5 The Screen Printing Deposition Technique of the Photo-electrode

Research in solar technology has indicated that the major challenge in the photo-electrode deposition methods is unequal thickness of the coatings. Screen printing method is a solution to the unequal thickness of the coatings by giving uniform coating and is used in the

industries to manufacture organic solar cells. These uniform coatings are achieved by extruding TiO_2 solution over a net of small pores.

Screen printing deposition method application is now widely used, apart from manufacture of organic solar cells, it is used in photo-voltaics to obtain thin-film CdTe solar cells (Sahnoun. 2015). Screen printing method is well embraced because of its key benefits. Among the key benefits are: it is simple therefore to use screen printing method deposits TiO_2 layer on the collection of the substrate simultaneously and is able to print the elements of DSSC film by film. The principle of surface tension creates desirable characteristics in screen printing because when TiO_2 is applied on the mesh, deposition results in a layer which has high surface roughness a feature very important in dye adsorption.

3.6 Counter-Electrode Coat

In order to maintain constant electron flow, the counter electrode is coated with a catalytic material such as carbon. This catalyst helps in the oxidation and reduction of the dye sensitizer. The carbon rod from an ordinary pencil can be said to be one of the easily available DSSC. The amorphous counter-electrode coating is achieved by depositing carbon on the surface of the conductive glass substrate. The deposition process is quite simple and is widely used in laboratories to explain simple DSSCs. The efficiency of solar cells made using this carbon is relatively high since it has small particles which increase surface area for converting tri-iodide back to iodide (Sahnoun. 2015).

The most usually utilized carbon in the DSSC is the residue from combustion flame. The counter electrode covering is accomplished by storing the sediment on the surface of the

conductive glass substrate. The procedure is very basic and is broadly utilized as a part of research facilities to clarify straightforward DSSCs. The effectiveness of sunlight-based cells influenced utilizing this carbon to ash is generally high since the residue has little particles which builds surface region for changing over tri-iodide back to iodide (Sahnoun. 2015).

The carbon sediment system normally endures a few mishaps in that the saved carbon coatings are delicate and a considerable measure of care is required in taking care of the whole procedure. Besides, the electrolyte set between the anodes and the coatings scatters in the entire framework because of surface strain and in the process, it washes the carbon ash into the electrolyte.

3.7 Solar Cell Parameters

3.7.1 Solar Cell I-V Characterization

The relationship between current and voltage of the solar cell are used to discuss photovoltaic cell performance. The current and voltage characteristics are as a result of sampling current versus voltage combinations with their respective load impedances. The photo-voltaic cell performance in principle is the output of the current versus voltage relationship when the solar cell is directly irradiated by sunlight. This experiment is achieved by exposing the photovoltaic cell to constant light while varying the peripheral capacity.

3.7.2 Short circuit current *(I_{sc})*

This is the highest current drawn from the cell when the voltage is zero. Mathematically, short circuit current is computed with zero voltage.

$$I_{(V=0)} = I_{sc}. \quad (3.4)$$

In summary, short circuit current is as a result of the onward bias curve and is maximum in the control quadrant. Short circuit current can also be defined as the current formed in the solar cell on the event by photon excitation.

In the forward bias process, the following relationship is true.

$$I_{sc} = I_{max} = I_1. \quad (3.5)$$

I_{max}- current at maximum power point.

I_1- load current.

3.7.3 Open Circuit Voltage (V_{oc})

With zero current flowing in the solar cell, we say the solar cell has open circuit voltage. This can be summarized as follows.

$$V_{(at\ I\ =\ 0)} = Voc \quad (3.6)$$

In principle, we can say open circuit voltage is maximum for onward bias curve in the power quadrant. This can be explained as in the equation below.

$$V_{oc} = V_{max}. \quad (3.7)$$

3.7.4 Maximum Power (P_{max})

Power in the solar cell can be computed along the I-V sweep that is in the power quadrant. The following equation can be used in the power computation.

$$P = IV \quad (3.8)$$

Maximum power occurs between short circuit current and open circuit voltage but at short circuit current and open circuit voltage, the value of power will be zero. In principle, maximum power has current and voltage values denoted as V_{mp} and I_{mp}.

3.7.5 Fill Factor

Fill factor measures the quality of the solar cell. Fill factor is the ratio of maximum power to theoretical power at the short circuit current and the open circuit voltage. Graphically, square like I-V sweep is more desirable in features and with an average range of about 75%.

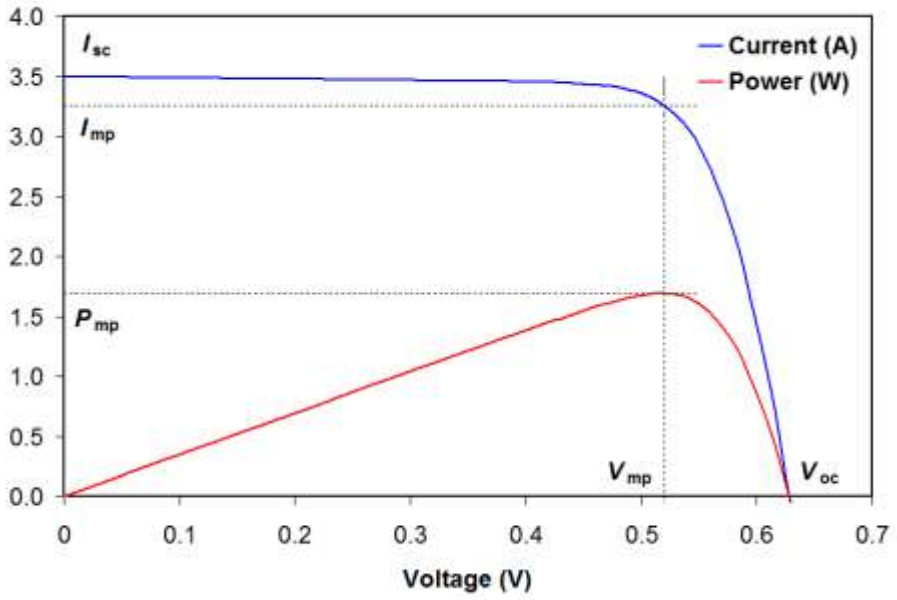

Figure 3.9: Maximum power of I-V sweep (Sahnoun *et al*., 2015).

Figure 3.10 provides equations and graphical representations for the following figures of merit: current ratio (dashed blue line), voltage ratio (dashed green line) and fill factor (green area÷ blue area).

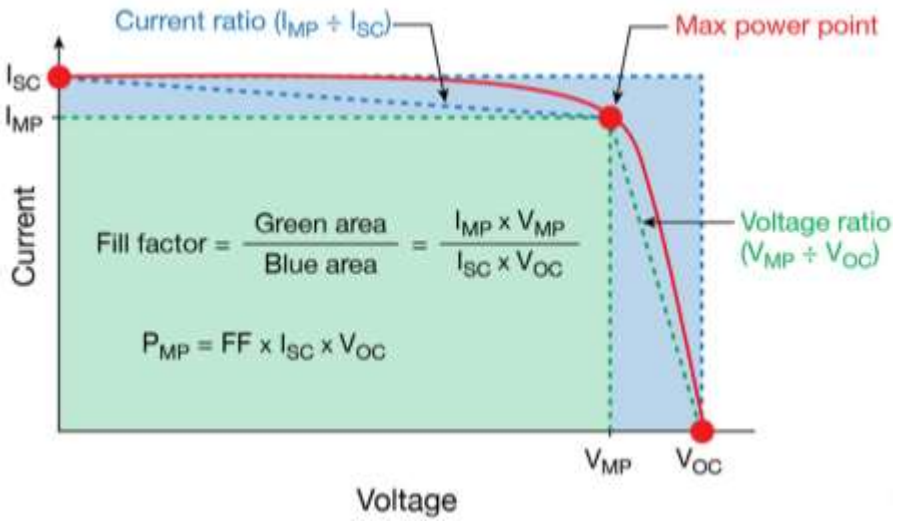

Figure 3.10: Fill factor from the I-V Sweep (Shakir *et al*., 2017)

3.7.6 Efficiency (η)

It is the ratio of electrical power output to solar power input in the photovoltaic cell. In principle, output power is sometimes referred to as maximum power because it can be operated up to the maximum power.

$$\eta = P_{out}/P_{in} = P_{max}/P_{in}. \quad (3.9)$$

Power input is regarded as the function of irradiance of the incident light. Power input is measured in W/m^2 where meter square is the surface area of the solar cell. It is discussed that ambient temperatures and intensity of the spectrum of the incident light affects the ability of the solar cell to achieve maximum efficiency. In principle, I-V parameters have direct effect on the performance of the solar cell and to do a comparison of the PV cells, same lighting and temperature conditions are needed.

Efficiency of photo-electrochemical cells greatly relies on the light absorbing dye sensitizer, electron transfer and electron regeneration. These three factors start by exciting the electrons and transferring the electrons into the conduction band of the nano-particle semi-conductor. It is estimated that electron transfer to the counter electrode takes place at a high efficiency hence the high overall efficiency of the solar cell. Iodide is converted to tri-iodide through the oxidation process at the dye sensitizer giving electrons to the positive charge carriers. Subsequent flow of electrons to the counter electrode reduces tri-iodide to the iodide through regeneration process.

Solar energy experts advise that to achieve maximum efficiency, the light must excite maximum number of electrons hence increasing the current generated, the dye sensitizer and the TiO_2 need to have a large surface area for maximum electron transfer and the chemical reduction and oxidation should occur at a rate higher than electron excitation.

3.8 Optical Description

3.8.1 Optical reflectance

The ratio of intensity of the incident light to that of the reflected light is what is called optical reflectance. In principle, incident light is shone on the surface having thin films and the subsequent intensity of the reflected light is measured the two are compared under reflectance.

$$R = \frac{I_r}{I_o} * 100 \qquad (3.10)$$

I_r- incident intensity.

I_o- reflected intensity.

3.8.2 Optical Transmission

In optical transmission, photons of definite wavelength and concentration are focused at the film. The transmission results in photons having energies greater than band gap energies to be absorbed and the lower energies are transmitted since this energy does not excite electrons to higher states. The ratio of the intensity of incident and transmitted photons is what is called transmittance.

$$T = \frac{I_t}{I_o} \tag{3.11}$$

3.8.3 Absorption of Light

Light is absorbed when photon of energy is able to excite an electron from lower to higher energy states. Light is normally absorbed when passing from one medium to another in the event that the photon has hit the film. It is by common sense that as light propagates, its relative intensity decreases hence the term absorption coefficient (ά). Equation 3.12 is the expression relating the incident photon (I_o), intensity of photon (I_t), film thickness (l) and the absorption coefficient (α).

$$I_t = I_o e^{-\alpha l} \tag{3.12}$$

Absorption of light entirely is affected by three main factors. These factors are: wavelength of the photon, film thickness, and film properties. In the event of photon energies happening

below band gap energy, absorption coefficient is rated zero. When the photon energy increase beyond the band gap energies the value of the absorption coefficient increases making the film not to allow any light to pass through for photon energies higher than the band gap energy (Shakir *et al.,* 2017). Absorption coefficient seeks to explain the depth light of certain wavelength can penetrate in the film before it is absorbed. Low absorption coefficient means poor light absorption and high absorption coefficient means better light absorption. The semiconductors used in the DSSCs have a sharp edge in absorption coefficient hence better light absorption (Sofyan *et al*., 2013). Light is assimilated when photon can energize an electron from lower to higher states.

CHAPTER 4

MATERIALS AND METHODS

4.1 Introduction

The conductive glass (fluorine doped tin oxide) substrates and titanium dioxide paste used in this work were purchased from solaronix. All the work of constructing and characterizing the solar cell was done in the physics laboratories at University of Nairobi.

4.2 Cleaning of substrates

The glass substrates of required thickness were purchased when they were already coated with fluorine doped tin oxide (FTO). The cleaning of the FTO conductive glass substrates was done in the ultrasonic bath. They were first cleaned in a detergent solution for 10 minutes, then rinsed with water and finally with ethanol and allowed to dry. The process of cleaning and drying was done at room temperatures.

4.3 Dye extraction

Four types of sensitizers were used in this study; carotenes, xynthophylls, anthocyanins and ruthenium. Three types: anthocyanins, carotenes and xynthophylls were chosen based on their attachment groups, while ruthenium was used as a control (Wong and Bhattacharya 2016). The three dyes were chosen because they are readily available, cheap and non-toxic. The dyes were extracted from their respective plants by the use of a blender, one at a time. The dyes were filtered and the filtrates used in their original form. Ruthenium dye was purchased in powder form. To dissolve ruthenium, 0.01188g was added to 20ml of ethanol

and electrically stirred for one hour, in a closed container so that ethanol does not evaporate and covered with black paper to prevent exposure to light because of its photosensitive nature. This was done to get the best concentration, which was 0.5mM.

4.4 Deposition of photo-electrode and counter-electrode coatings

4.4.1 Screen printing on the photo-electrode

There are many ways of depositing a semiconductor on a substrate; spray pyrolysis, doctor blading, screen printing, among others. The latter was used in this study. The square cut FTO glass was placed beneath the mesh opening of the screen, with its conductive side facing up. The conductive side was determined using a multi-meter. The paste was scooped using a plastic spatula from its bottle, placed besides the mesh. A squeegee was then used to force the paste through the mesh. The mesh was gradually lifted from the screen after printing techniques of titanium dioxide coating. From the research, titanium dioxide did not separate from the mesh smoothly as expected. The abnormality of separation was due to surface tension between the substrate and the mesh. However, surface tension was useful in absorbing the dye for it created a rough surface (Mawyin, 2009). The deposited paste was allowed to dry at room temperature for five minutes and was heated on a hot plate at temperature 120^{o}C to evaporate the volatile liquids in the paste. The screen and the squeegee were then cleaned with acetone ready for another use.

4.4.2 Graphite coating on the counter-electrode

Graphite was used because it is a catalyst that is readily available, non-toxic and easy to apply. Carbon was rubbed on the conductive side of the FTO glass to make a counter-electrode. Rubbing was done several times to ensure even distribution of the catalyst.

4.5 Annealing and sintering of the deposited layers

Annealing is the heat treatment to a specified temperature and then cooling at a controlled rate for cold working conditions. For 10 minutes TiO_2 was preheated at 120^oC and annealed in an open furnace, where temperature was increased in steps of 50^0 to manage thermal stress. A maximum value of 450^0 was chosen so that the TiO_2 does not change from anatase to rutile which is thermally stable. Annealing was necessary to burn inorganic components of the TiO_2 paste and also to improve the mechanical contact of the nonporous TiO_2 particles (harden on the substrates).The deposited paste on the FTO glass was carefully placed into the furnace. It was also essential to bind the paste on the FTO substrate and evaporate the volatile liquids in the paste. Sintering involves heating loose fine particles into compact solid or porous mass. Sintering was done so as to create pores for the percolation of the electrons during the working of the cell (Seige *et.al*, 2006).

4.6 Sensitization of TiO_2 substrates

The annealed and sintered TiO_2 substrates were sensitized for 18 hours. The TiO_2 substrates were removed from the furnace at a temperature of 80^0C and immediately immersed inside the respective dyes. This was done to ensure maximum adsorption of the dye on the TiO_2 semiconductor. After the sensitization period was over, the photo-anodes were removed

from the dye solutions. The thin films were cleaned in de-ionized water and then in propanol to remove any excess water. Some of the thin films were kept in a clean container for solar cell assembly and others were taken for optical characterization.

4.7 Optical characterization

The shimadzu model type DUV3700of UV-VIS-NIR spectrophotometer was used to characterize thin films. This was done at normal irradiance that is perpendicular. Optical transmittance and reflectance for the three organic and ruthenium dyed thin films were measured. The optical absorbance for the same dyed thin films was calculated. Microcal Origin Lab software was used to plot the graphs of transmittance, absorbance and reflectance.

4.8 Cell Assembly

The previously prepared electrodes (in 4.4.1 and 4.4.2 subsections) were put together with the conductive sides facing one another. A scotch tape was cut out and the central part the size of the active area of the photo anode cut out. It was introduced between the two electrodes and heated at a temperature of 100^0C so that it melts to bind the electrodes together. The uncoated offsets were left hanging and used as electrical contacts. The iodine electrolyte was introduced between the two electrodes through a hole of 1mm in diameter, and spread uniformly by capillarity. Any excess electrolyte was dried using a blotting paper. The hole on the counter electrode was sealed so that when it is turned to be the base, the electrolyte should not leak.

4.9 I-V characterization of the DSSCs

4.9.1 Diode characteristics

The solar cell I-V characteristics were determined using the Keithly 2400 source meter. The source meter was interfaced with the computer with the help of lab view programs. The diode characteristic parameters were also calculated using the lab view program. The Keithly 2400 source meter used contained 4 sensitive probes for purposes of high precision (2 for current and 2 for voltage). Two probes were connected to the counter electrode while the other two probes on the photo-anode and the signal was transmitted to the Keithly source meter. The source meter then sent the signal to the computer fitted with lab view program.

CHAPTER 5

RESULTS AND DISCUSSION

5.1 Introduction

In this chapter, optical and electrical characteristics are presented. The optical values were found by fitting the spectra with theoretical oscillator models in the scout 98 software. This chapter discusses the characteristics of the solar cell including the short circuit current (Isc), Fill Factor (FF), Open circuit voltage (Voc), maximum current (Imax), maximum output voltage (Vmax) and conversion efficiency (η)

5.2 Optical Results

The optical results of transmittance and reflectance were measured in the range of 200-2500 nm wavelength. Other optical properties like absorption were calculated using the Scout software. Figure 5.1 shows percentage transmittance against wavelength in nanometers for the single dyed thin films. It can be seen from the graph that thin films transmit in the visible and near infra-red range. Much emphasis was on the visible range because this is the desired region for solar cell operation.

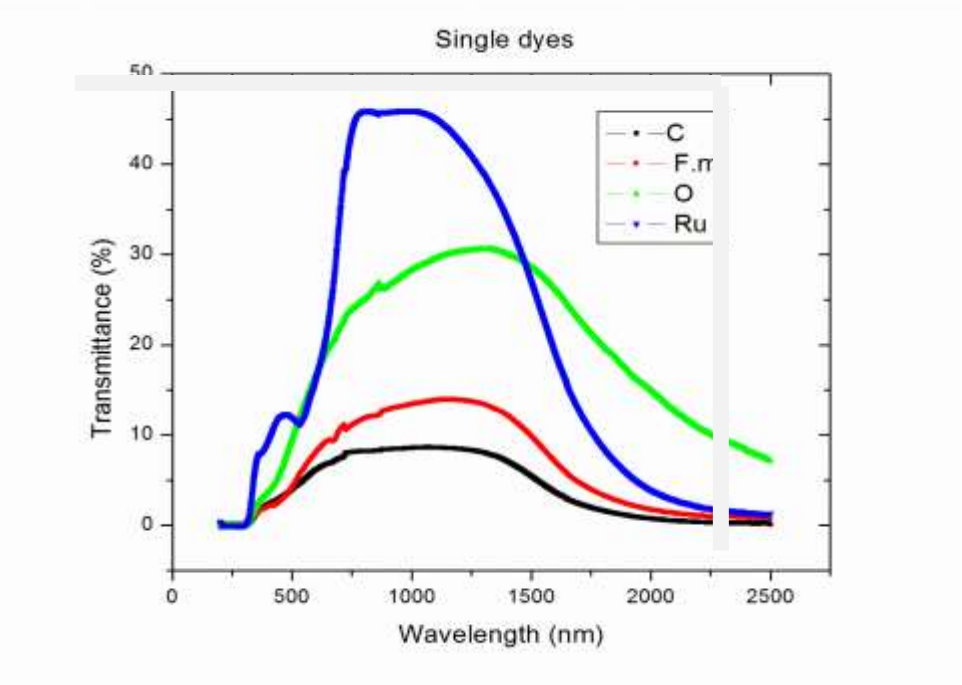

Figure 5.1: Transmission characteristics of single dyes.

From the graph of figure 5.1 the peak transmittance of the different dyes were determined and results tabulated as in table 5.1.

Table 5.1: Transmittance peaks of single dyed thin films

Dye	Percentage Transmittance (%)	Wavelength (nm)
Carrot (c)	8	1000
French marigold (F.M)	11	1000
Orange (O)	30	1250
Ruthenium (Ru)	47	800

.

The graphs in figure 5.1 show different values of transmittance. At low wavelengths of the visible range the transmittance was low. From 500nm transmittance increased up to a wavelength of 780nm after which it remained constant. Beyond 1000nm the transmittance values started dropping. Carrot dye transmitted at a peak of 8%, French marigold dye transmitted at a peak of 11% while Orange dye transmitted at peak of 30% and ruthenium dye transmitted at peak of 47% in the range of 200-2500 nm. This was attributed to the –OH bonding in the carrot dye and French marigold dyes. Ruthenium has a lot of benzene rings which are symmetrical, unlike orange dye which had the asymmetrical 3 benzene rings. Ruthenium dye and orange dye transmitted the most unlike carotenes which have carboxyl groups and xynthophylls which have hydroxyl groups for attachment onto the semiconductor. The transmittance of each organic dye and its dye mixture was then studied.

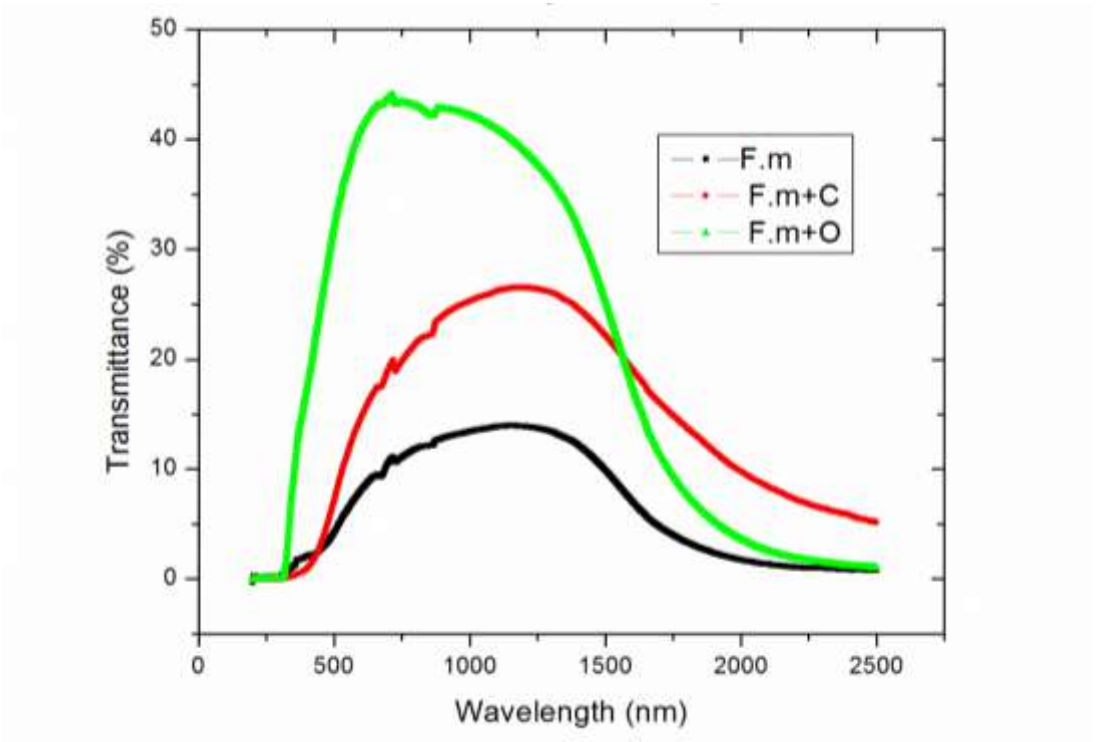

Figure 5.2: Transmission characteristics of French marigold dye and its dye mixture.

From the graph in figure 5.2, it was observed that mixing French marigold dye with either carrot dye or orange dye increased the peak transmittance. These increased transmittances of the dye mixtures implies that the amount of energy absorbed was decreased. This was attributed to the vibration of their chemical groups as they interact. Table 5.2 shows the peak percentage transmittance versus wavelength in nm of French marigold dye coated thin film and how it compares with its dye mixtures.

Table 5.2: Transmittance peak of French marigold dye and its dye mixtures

Dye	Percentage transmittance (%)	Wavelength (nm)
French marigold	14	1000
French marigold and carrot	26	1000
French marigold and orange	44	560

When the carrot dye was mixed with French marigold dye and also with orange dye, the peak transmittance for the dye mixtures was higher than that of carrot dye. The mixture of carrot dye and orange dye transmitted the most from the graphs in Figure 5.3. This was attributed to the difference in their chemical structures as they interact.

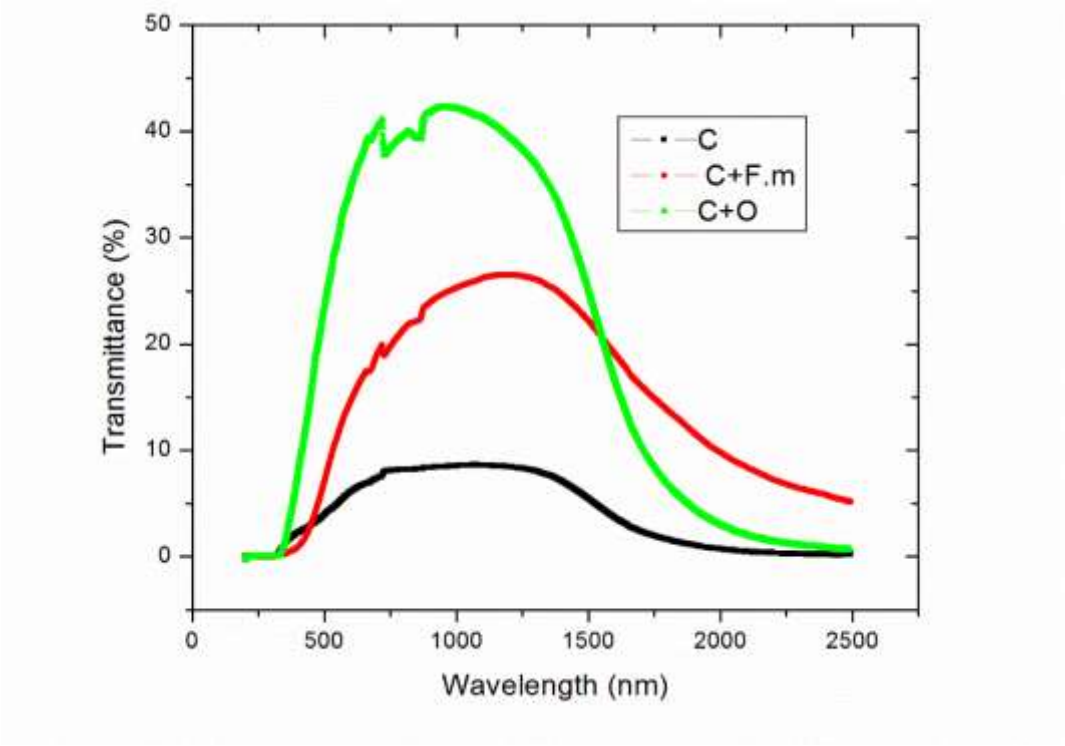

Figure 5.3: Transmission characteristics of carrot dye and its dye mixtures.

The peak transmittance for the carrot dye and peak transmittance for its dye mixture are tabulated in table 5.3. Table 5.3 shows the peak percentage transmittance against wavelength in nm of carrot dyed thin films and how it compares with its dye mixture in the range of the spectrum.

Table 5.3: Transmittance peak of Carrot dye and its dye mixtures.

Dye	Percentage transmittance	Wavelength (nm)
Carrot	6	1000
Carrot and French marigold	25	1250
Carrot and Orange	40	900

Mixing of the dyes in all cases increased the peak transmittance than single dyes. This was attributed to surface interactions on the semiconductor. Furthermore, the presence of symmetric and anti-symmetric –CH stretching vibration modes of CH_2 and CH_3 groups in their chemical structures respectively could have been a major contributing factor.

When the orange dye was compared with its dye mixtures, the graphs were as in figure 5.4. Orange dye transmitted less than its dye mixtures across all wavelengths which can be attributed to the fact that mixing increased the surface interactions which consequently increased the peak transmittance.

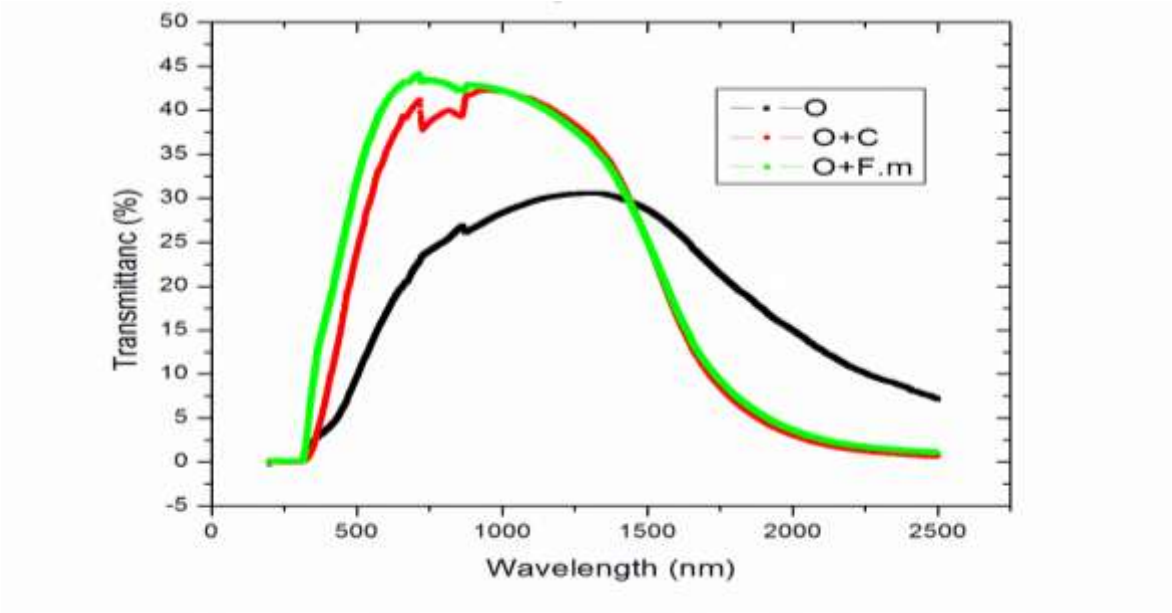

Figure 5.4: Transmission characteristic of Orange dye and its dye mixtures

Among the organic dyes, orange dye transmitted the most. This was attributed to the asymmetrical benzene rings in the chemical structure of orange dye. Table 5.4 represents the peak percentage transmittance against wavelength of Orange dyed thin films and how it compares with its mixtures.

Table 5.4: Transmittance peaks of orange and its dye mixtures

Dye	Percentage transmittance	Wavelength (nm)
Orange	30	1250
Orange and Carrot	42	800
Orange French marigold	43	620

The transmittance for the mixtures were then plotted against wavelength. For comparative purposes, Ruthenium was plotted on the same axes.

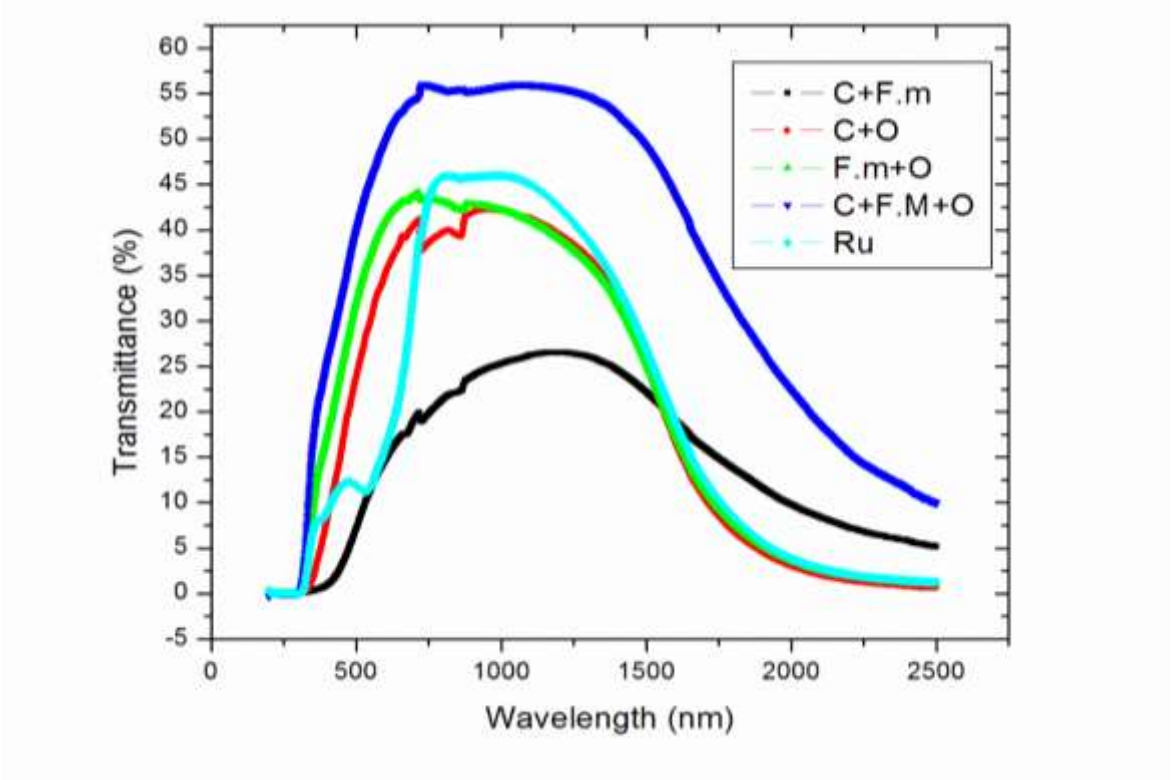

Figure 5.5: Transmission characteristics of the dye mixtures and ruthenium

It was observed that the mixture of the three organic dyes transmitted higher than ruthenium dye. It was concluded that as the number of dyes mixed increased from two to three,

percentage transmittance also increased. This was attributed to more dye particles interacting on the surface of the semiconductor.

Table 5.5 shows the comparison of the peak transmittance of mixed organic dyes with ruthenium dye and their wavelength in the spectrum.

Table 5.5: Comparison of peak transmittance of mixed dyes and ruthenium dye.

Dye	Percentage	Wavelength nm
Carrot and French marigold	27	1000
Carrot and Orange	40	900
French marigold Orange	42	600
Carrot, French marigold and Orange	55	820
Ruthenium	45	750

Apart from transmittance, another optical characterization that was measured was reflectance. When the percentage reflectance was plotted against wavelength in the range of 200-1250nm, the peak reflectance was as in figure 5.6.

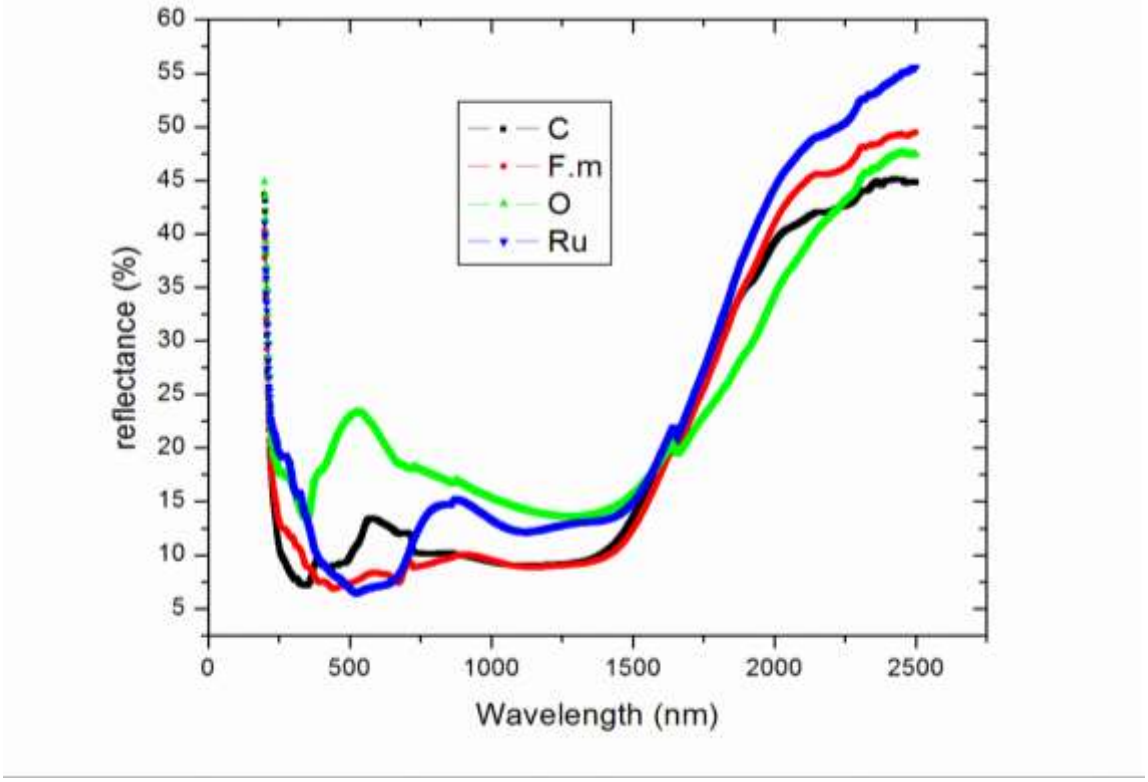

Figure 5.6: Reflectance peak characteristic of the single dyes thin films**.**

The peak reflectance values in the range 200-1250 nm for the organic dyes and ruthenium dye were tabulated as in table 5.6.

Table 5.6: Reflectance peak characteristic of the single dyes.

Dye	Percentage reflectance	Wavelength (nm)
Carrot	14	600
French marigold.	8	610
Orange	24	590
Ruthenium	15	900

From the graph, it is evident that for 200nm-1250nm, orange dyed thin film reflects the most because of its chemical structure that has benzene rings unlike the carrot dye and French marigold dye which have carboxyl groups to attach to the semiconductor. This gives a projection that the conversion efficiency of orange dye might be lower than the rest of the thin films in this work.

Absorbance was another important parameter. It was calculated from the results of transmittance and reflectance, in the range of 200-2500nm. The graphical representation of absorbance is shown in figure 5.7.

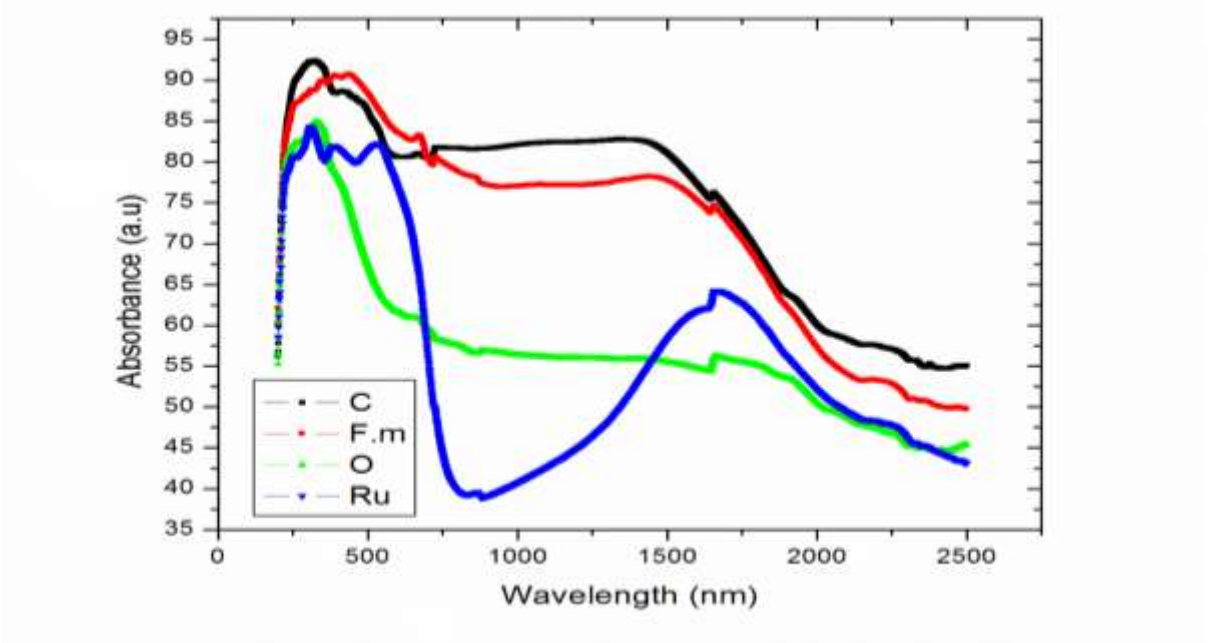

Figure 5.7: Absorption characteristics of single dyed thin films.

From the graph, it was observed that the peak absorbance was 92% for carrot dye and a peak of 91% absorbance for the French marigold dye. Carrot dye has the carboxyl groups in its chemical structure that bonded strongly on the semiconductor. Likewise, for the French

marigold dye which has the hydroxide groups that bonded strongly with the TiO_2.The oxide groups in the orange dye formed a weak bond with TiO_2. This explains why the peak absorbance for the orange dye was lower (85%). Ruthenium dye absorbed at a peak value of 84%, close to the orange dye. However, the absorption peak for the ruthenium dye was broader than that of the orange dye. Ruthenium had a wider absorption because of its symmetrical benzene rings that formed very strong bonds on the semiconductor. Orange dye had asymmetrical benzene ring that formed weak bonds with the semiconductor. After 650nm the absorption shifted to lower energy. This was attributed to complexion between the dyes and the metal oxides. The absorption peaks were found to be in the visible range. Table 5.8 shows the absorption characteristic of mixed dyes thin films and how they compared with ruthenium dye thin film.

.

Table 5.7: Absorption peak characteristics of single dyed thin films.

Dye	Percentage absorption	Wavelength (nm)
Carrot	92	300
French marigold	91	420
Orange	85	380
Ruthenium	84	385

When the organic dyes were mixed in the ratio of 1:1 by volume, and their absorbance calculated, they gave the results as in figure 5.8.

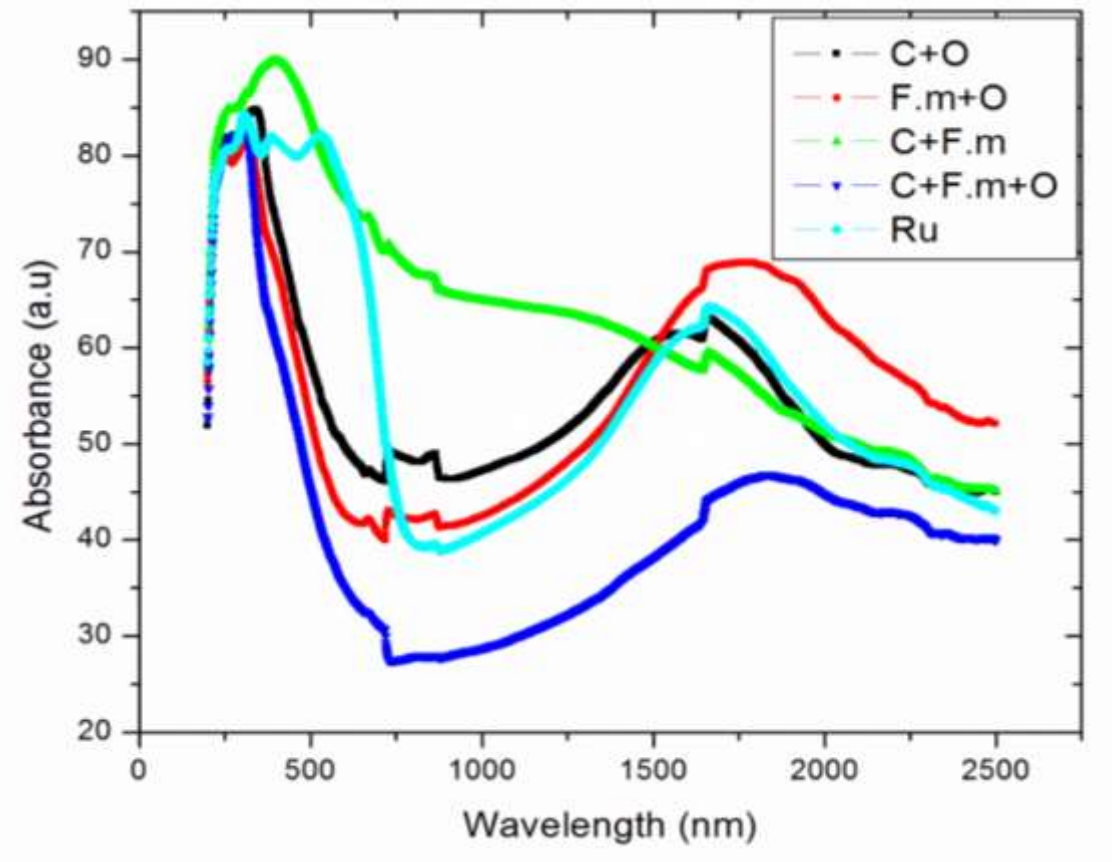

Figure 5.8: Absorption characteristics of mixed dyed thin films.

For an average wavelength of 580nm of the visible range, the mixture of carrot dye and French marigold dye thin film competes with ruthenium dye thin film for the absorption peaks. This was attributed to the good attachment sites to the semiconductor material. This can be seen from figure 5.8. From figure 5.8, it was observed that the mixture of carrot dye and French marigold dye had the peak absorption at 580nm because of the presence of hydroxide and the carboxyl groups in their chemical structures than the asymmetrical benzene rings in the chemical structure of the anthocyanins. From figure 5.8 it was

concluded that different dyes have different abilities to absorb light energy at different wavelengths in the visible range. The absorption peaks from figure 5.8 were tabulated as seen in table 5.8.

Table 5.8: Absorption peak characteristics of organic dye mixtures and ruthenium.

Dye	Percentage absorption	Wavelength (nm)
Carrot and Orange	85	375
French marigold and Orange	82	380
Carrot and French marigold	90	515
Carrot, French marigold and Orange	82	300
Ruthenium	84	375

5.4 IV characterization of DSSC

5.4.1 Dark I-V characteristics

Figure 5.9 is the representation of I-V features of the DSSC. From the figure, it can be seen that a DSSC behave like a p-n junction diode. The efficiency of the organic dyes was fairly good. They have a narrow spectral absorption range, some have low energy levels for electron transfer to TiO_2 (Gratzel, 2003). From table 5.9, it can be seen that carrot dye gave the highest efficiency of 0.100. This was attributed to its high viscosity. When the temperature increased (during the annealing process), it facilitated the permeation of the dye solution into the electron carrier which essentially covered a large surface area and improved the efficiency of the cell (Zhu *et. al*, 2010). The low short circuit current may be attributed

to the incompatibility between the energy of the excited state of the adsorbed dye and the conduction band edge of the TiO_2 (Zhu *et. al*, 2010). Anthocyanins (Orange) dye DSSC gave the least efficiency of 0.087%. This was attributed to high rate of recombination and the various competitive processes in the cell. Also its narrow absorption of the spectrum in the visible. Figure5.9 gives the I-V characteristics of the single dyed organic thin film DSSC.

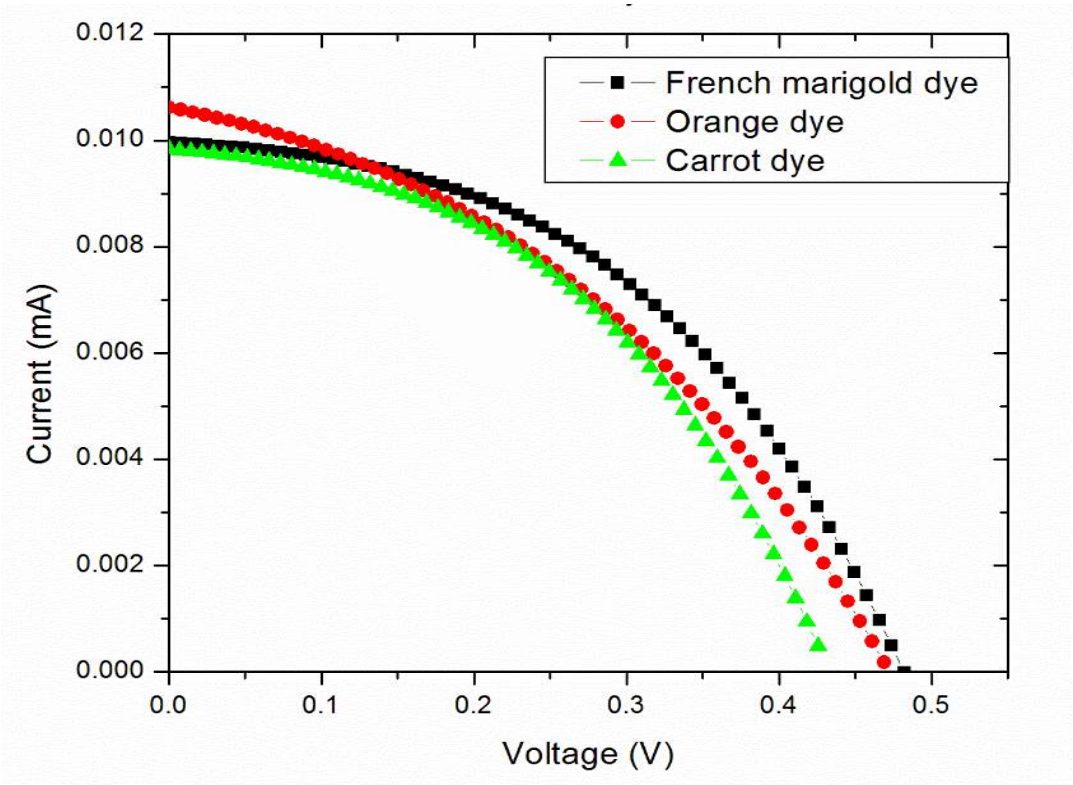

Figure 5.9: I-V Characteristics of DSSC of single dyed thin films.

From the graph in figure 5.9, Table 5.9 was tabulated to give the I-V characteristics of single dyed thin films.

Table 5.9: I-V characterization of single dyed thin films.

	V_{oc}	Isc (mA)	FF (%)	I_{MAX} ($mAE-^{5}$)	V_{MAX}	P_{MAX} $(W)E^{-5}$	*Ƞ(%)*
Carrot	0.482	0.0092	69.8	1.063	0.452	4.809	0.100
F.M	0.469	0.0099	69.3	1.060	0.439	4.655	0.097
Orange	0.433	0.0100	67.1	1.042	0.403	4.200	0.087

When the single dyes were mixed with other dyes to see the effect on the I-V characteristics, it was observed that their efficiencies were slightly lowered. This was attributed to the surface interactions on the TiO_2.

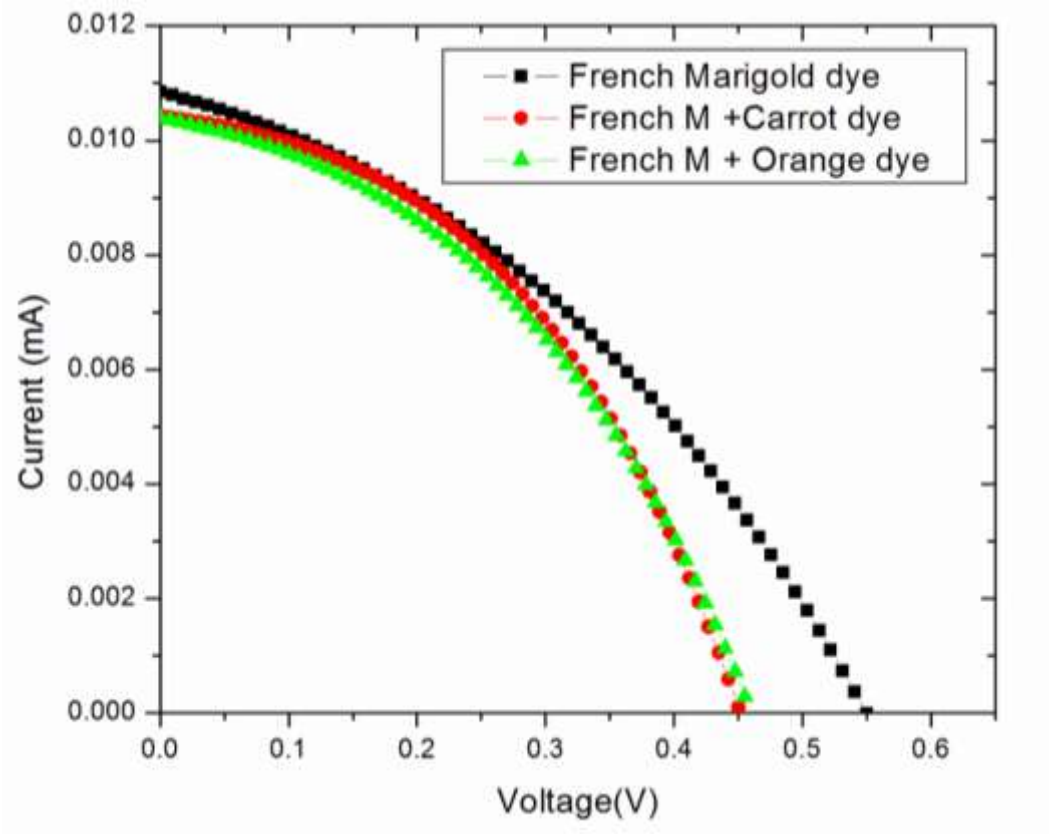

Figure 5.10: I-V characteristics of DSSC of French Marigold dye and its dye mixtures.

The increased surface interaction, increased the transmittance of the dye mixtures and lowered the energy absorbed to cause photo-excitation. The intensity of incident light and potential of the cell determined the amount of current produced by the cell. At zero potential, current was maximum (I_{sc}) and as the potential increased, the current flux decreased. Table 5.10 gives the summary of the electrical characteristics of French Marigold DSSC and its dye mixtures.

Table 5.10: I-V summary for French marigold and its mixtures

	V_{oc}(V)	I_{sc}(mA)	FF (%)	I_{MAX}(mA)E^{-5}	V_{MAX}(V)	P_{MAX}(W)E^{-5}	η (%)
F.M	0.469	0.0099	69.3	1.060	0.439	4.655	0.097
F.M+C	0.450	0.0101	67.8	1.049	0.420	4.404	0.092
F.M+O	0.454	0.0102	67.1	1.040	0.424	4.410	0.092

Figure 5.10 shows the I-V characteristics of DSSC of French Marigold dye DSSC and its mixtures in visible range. At maximum potential the short circuit current is zero. The maximum potential for french marigold dye is higher than that of its dye mixtures. This was attributed to mixed interactions on the surace of the semiconductor. The low efficiency of the French marigold dye was attributed to its peak absorbance of the long wavelength that was less energetic to excite the electrons.The mixtures gave slightly lower efficiencies than the single dye of French marigold dye. This was attributed to the narrow spectrum absorption.

Among the three organic dyes researched on, carrot emerged the best on the optical performance and even the I-V properties. The dye was further investigated by mixing it with other organic dyes in the ratio of 1:1 by volume. The I-V characteristics of the carrot dye and its organic dye mixtures are as shown in figure 5.11.

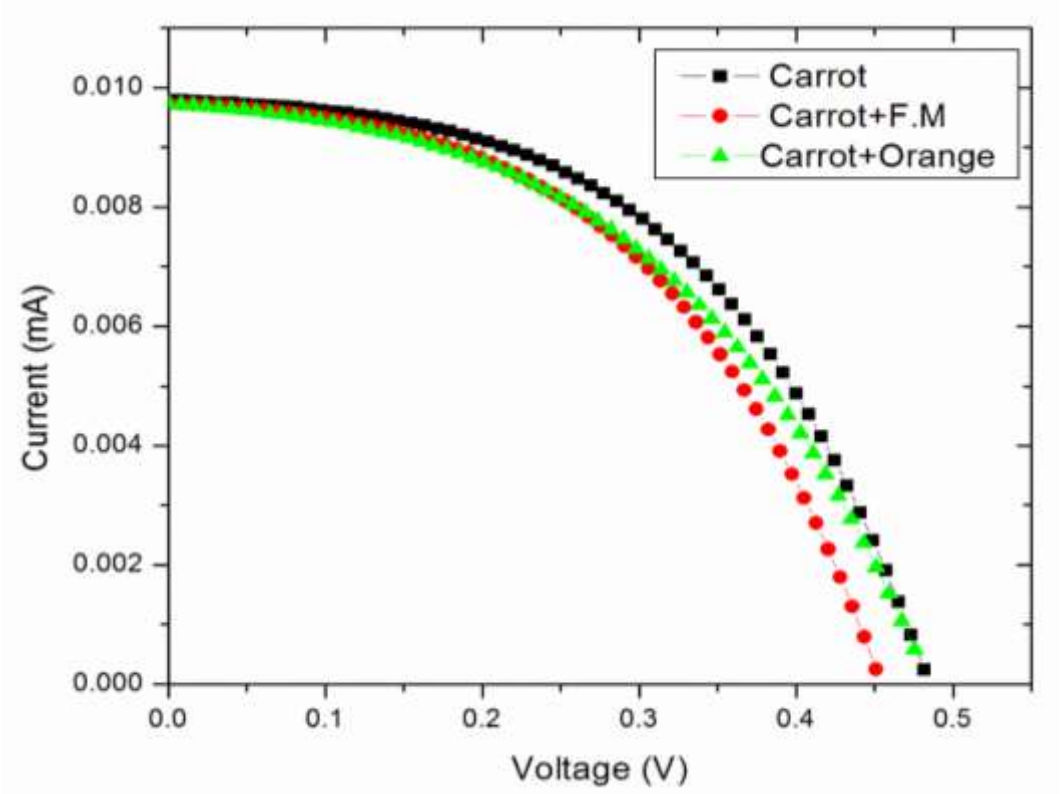

Figure 5.11: I-V characteristics of DSSC. of carrot dye and its dye mixtures.

The I-V parameters from figure 5.11 were tabulated as in table 5.11 for the carrot dye and its dye mixture thin films.

Table 5.11: I-V summary of carrot dye and its dye mixtures.

	V_{oc} (V)	I_{sc} (mA)	FF(%)	I_{MAX} (mA) E^{-5}	V_{MAX} (V)	P_{MAX} (W)E^{-5}	η (%)
Carrot	0.482	0.0092	69.8	1.063	0.452	4.809	0.100
C+F.M	0.450	0.0101	67.8	1.049	0.420	4.404	0.092
C+O	0.468	0.0098	69.4	1.061	0.438	4.648	0.099

Carrot out performed the other two organic dyes. Addition of the other organic dyes into the carrot lowered its conversion efficiency. This was attributed to the many CH_3 groups in its structure to chemically adsorp on the semiconductor. It was also noted ealier that carrot transmits less than the other two organic dyes.

Orange dye was one of the organic dyes. It emerged that it was very different from other organic dyes in that it was the only one with benzene rings in its chemical structure. It also transmitted the most and absorbed the least in the visible range. The I-V characteristics of the orange dye and its dye mixtures are as shown in figure 5.12.

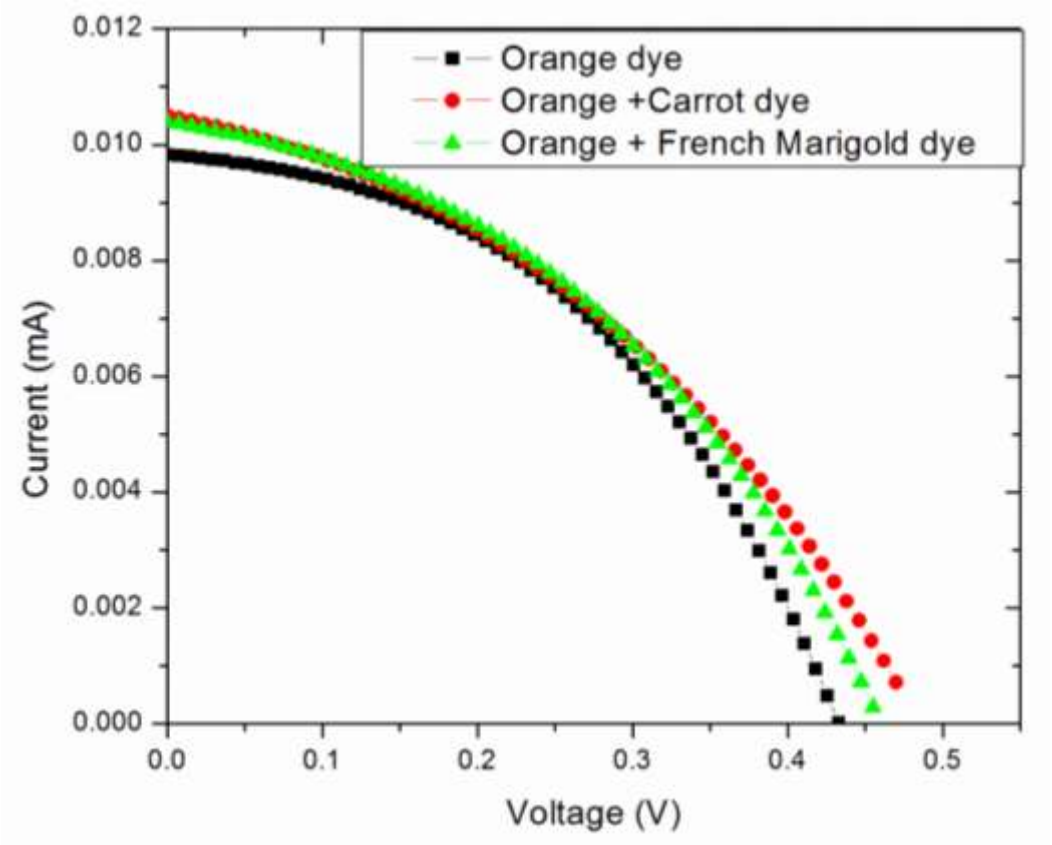

Figure 5.12: I-V characteristics of DSSC of Orange dye and its dye mixtures.

Mixing the orange dye with the other organic dyes improved the cell performance. From the graph, it was observed that the values for Isc and Voc for the dye mixtures were higher than that of orange dye alone. The power output for the mixed DSSC also improved, see table 5.12.

Table 5.12: I-V summary of orange dye and dye mixtures.

	Voc(V)	Isc (mA)	FF (%)	I_{MAX} (mA) E^{-5}	V_{MAX}(V)	P_{MAX} (W) E^{-5}	*Ƞ (%)*
Orange	0.433	0.0089	67.1	1.042	0.403	4.200	0.087
O+C	0.468	0.0101	69.4	1.061	0.438	4.648	0.099
O+F.M	0.454	0.0102	67.1	1.040	0.424	4.410	0.092

From figure 5.12, there is no forward current at zero bias. The forward current rises steadily. As the forward current increases to thin depletion layer, there is a steady rise of the forward current. The presence of the thin depletion layer is to allow charge carriers to flow across the p-n junction and as a result reducing the resistance.

- The DSSCs have different dyes on the titanium dioxide films. It was indicated that open circuit voltage and short circuit current were different for the different dyes. When efficiency was calculated using the formula,

$$\eta = \left(\frac{J_{sc}V_{oc}FF}{GA}\right) X100 \qquad (5.1)$$

it was found that the carrot dye solar cell had the highest value in the matrix, 0.100% and the orange dye solar cell had the least efficiency, of 0.087%. Cells that were sensitized by the mixture of the pigments had a better efficiency of 0.108%, and this was attributed to anchoring property of the dye on the semiconductor and wide range of absorption in the spectrum. These improved output performance of the dye mixtures is shown by figure 5.13.

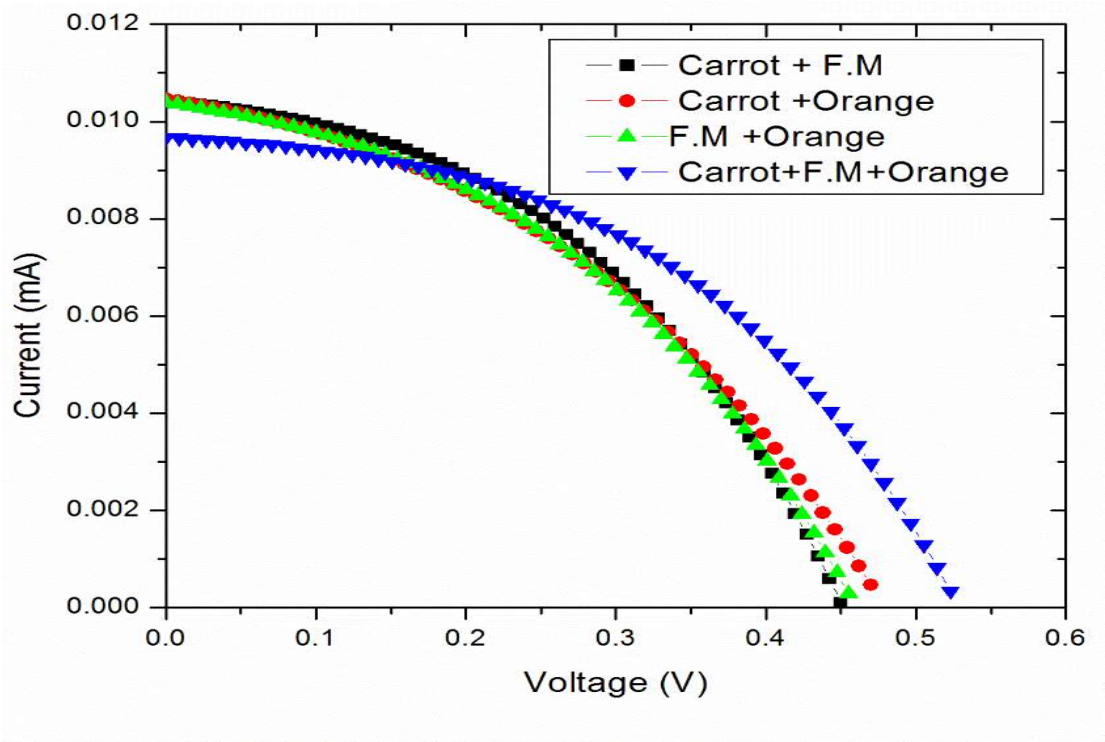

Figure 5.13: I-V Characteristics of DSSC of the organic dye mixtures

The summary of the I-V characteristics for the dye mixtures used in the DSSC is shown in table 5.13.

Table 5.13: I-V Summary of dye mixtures.

	V_{oc}(V)	I_{sc}(mA)	FF (%)	I_{MAX}(mA)E^{-5}	V_{MAX}	P_{MAX}(W)E^{-5}	*Ƞ (%)*
C+F.M	0.450	0.0101	67.8	1.049	0.420	4.404	0.092
C+O	0.468	0.0098	69.4	1.061	0.438	4.648	0.099
F.M+O	0.454	0.0102	67.1	1.040	0.424	4.410	0.092
C+F.M+O	0.523	0.0097	69.2	1.053	0.493	5.159	0.108

Although the mixture of the three organic dyes gave a better efficiency, ruthenium, which was used as a control experiment gave the best as expected. It gave an efficiency of 1.032% which was ten times more than the organic dyes. This was attributed to its wide range of absorption in the spectrum high anchoring property, high stability and optimum Redox potential high absorption coefficient (Seige *et. al*, 2006). This was observed in its high value of short circuit current of 0.1950mA, unlike the organic dyes that had a short circuit current in the range of 0.0092-0.0102mA. This low short circuit current in the local DSSC was attributed to electron-hole recombination since they were water soluble unlike the ruthenium dye cell which was dissolved in alcohol, a better conductor than water. Figure 5.14 below show the I-V curve for ruthenium dye.

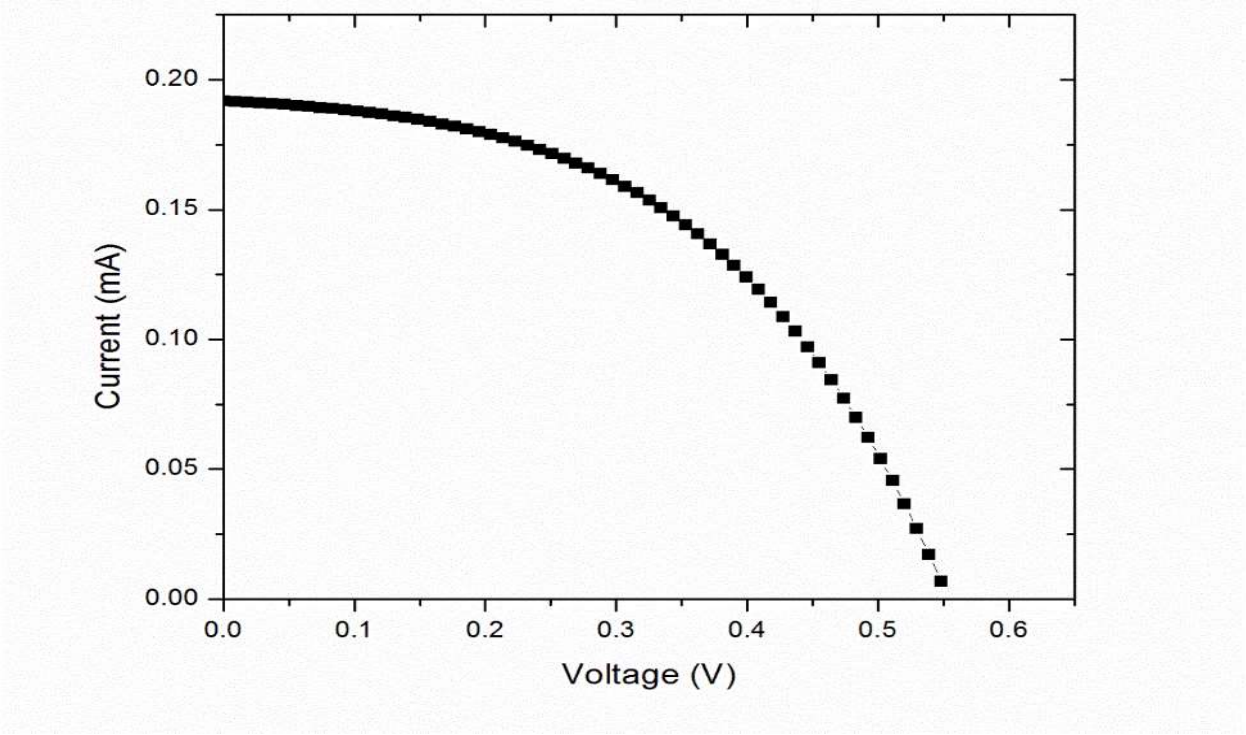

Figure 5.14: I-V Characteristics of ruthenium dye

The density of injected electrons have a direct influence on the conductivity of the titanium dioxide and the chemical structure of the dye in principle, the performance of the solar cells greatly relies on the type of dye used.

This difference is because of the wide absorption ability of the ruthenium dye nearest to the region of infrared. In principle, ruthenium sensitizers have a steady electrode injection compared to oxidized sensitizers. Secondly, ruthenium has a high optical cross-section which is a desirable feature for high light harvesting as compared to other sensitizers. In summary, HOMO and LUMO energy levels determine the ruthenium absorption spectra in the polypyridyl systems (Nazerruddin and Mohammed, 2007). The summary of all the I-V characterization of all the DSSCs is compared in table 5.14.

Table 5.14: Summary of all the I-V characteristics of all the dyes.

	V_{OC} (V)	I_{SC} (mA)	FF (%)	I_{MAX}(mAE^{-5})	V_{MAX} (V)	P_{MAX} (W) E^{-5}	Efficiency (%)
Carrot	0.482	0.0092	69.8	1.063	0.452	4.809	0.100
F.M	0.469	0.0099	69.3	1.060	0.439	4.655	0.097
Orange	0.433	0.0100	67.1	1.042	0.403	4.200	0.087
C+F.M	0.450	0.0101	67.8	1.049	0.420	4.404	0.092
F.M+O	0.454	0.0102	67.1	1.040	0.424	4.410	0.092
C+O	0.468	0.0098	69.4	1.061	0.438	4.648	0.099
C+O+F.M	0.523	0.0097	69.2	1.053	0.493	5.189	0.108
Ruthenium	0.565	0.1950	58.1	1.321	0.415	5.485	1.032

From table 5.14, it was concluded that the maximum open circuit voltage output was obtained from the ruthenium dye 0.565 volts and the least open circuit voltage was obtained from the orange dye solar cell. The values of the fill factor was on average 68%, which describes the quality of the solar cell characterized. The value was less than 100% due the parasitic conditions. Internal resistances of the solar cell reduces the amount of the power out. The series resistance is caused by either the bulk substrate or the metal contacts in the circuit. It is calculated by getting the reciprocal of the slope near the open circuit voltage. The series resistance has no effect on the V_{oc} since the current is zero. Impurities in the cell lead to the leakage of the current, which causes the shunt resistance. It is obtained by the inverse of the slope near the I_{sc}. A high value is necessary so that all the current generated flows in one direction. High value of R_{SH} is good for the efficiency and maximum power output.

CHAPTER 6

CONCLUSIONS AND RECOMMENDATIONS

6.1 Conclusions

The extraction of the organic dyes by use of a blender was successful. Paste deposition by screen printing technique was done. Fabrication of the thin films using anthocyanin, carotene, xanthophylls and ruthenium dyes was done. Optical characterization using a DUV 3700 spectrophotometer was successful. The most transmitting thin film was the one made of orange dye. The most absorbing thin film was the one of carrot dye among the organic dyes. From the research, ruthenium dye gave the highest open circuit voltage values (565mV) whereas orange dye gave the lowest open voltage value (433mV). The short circuit current was 195 micro amperes from ruthenium and 9.2 microamperes from the carotene DSSC. This resulted to an average fill factor of around 67%. Efficiency was also noted to be averagely 0.2133%. We therefore conclude that DSSC should have dyes that have better anchoring property and low quenching effect for it to achieve the best I-V output characteristics and efficiency. We noted that the best natural dye to be used was carrot dye since it had relatively higher efficiency of 0.100% than orange dye and French marigold dye. Mixing the dyes for sensitization improved the cell efficiency (0.108 %) than the single dyed solar cell efficiency.

It was also observed that among the organic dyes, orange dye transmitted more followed by French marigold dye then carrot dye. Ruthenium dye transmitted the most. About absorption, carrot dye absorbed more than the rest of the dyes in the visible range i.e.380nm-780nm. A

dye that absorbs more transmits less. From the absorption curves ruthenium dye had wide range of absorption than the organic dyes in the visible range.

6.2 Recommendations

It is recommended that poly-ethylene glycol be obtained in future experiments to sufficiently bind the titanium dioxide nano-particles together to ensure thinnest films which produce more desirable current- voltage output characteristics.

6.3 Further research

In future more research need to be done on carrot as dye since from the three organic dyes used, it gave the best efficiency. It was used in its natural form without any additives or purifications. Ways of purifying the dye before sensitization to remove any impurities that may be present, which may contribute to recombination need to be looked at. There is also need to vary the thickness of TiO_2 with different dye concentration and compare the efficiencies.

REFERENCES

Allen, T. G., Bullock, J., Jeangros, Q., Samundsett, C., Wan, Y., Cui, J., & Cuevas, A. (2017). A low resistance calcium/reduced titania passivated contact for high efficiency crystalline silicon solar cells. *Advanced Energy Materials*, *7*(12), 1602606.

Anderson, D., Sankovic J., Wiltz D., Abelson R., Feurial J. and 2007 IEEE Aerospace Conference. (2007). NASA's Advanced Radioisotope power Conversion technology development status. *IEEE Aerospace Conference, (pg 1-20).*

Bube, R. H. (1998). Photovoltaic materials. London; Imerial College Press.

Chou, C. C., Wu, K. L., Chi, Y., Hu, W. P., Yu, S. J., Lee, G. H., ... & Chou, P. T. (2011). Ruthenium (II) Sensitizers with Heteroleptic Tridentate Chelates for Dye-Sensitized Solar Cells. *Angewandte Chemie International Edition*, *50*(9), 2054-2058.

Chen, C. Y., Wu, S. J., Li, J. Y., Wu, C. G., Chen, J. G., & Ho, K. C. (2007). A new route to enhance the light-harvesting capability of ruthenium complexes for dye-sensitized solar cells. *Advanced materials*, *19*(22), 3888-3891.

Feihl, S., Costa, R. D., Brenner, W., Margraf, J. T., Casillas, R., Langmar, O... & Guldi, D. M. (2014). Integrating metalloporphycenes into p-type NiO-based dye-sensitized solar cells. *Chemical Communications*, *50*(77), 11339-11342.

Grätzel, M. (2006). Photovoltaic performance and long-term stability of dye-sensitized meosocopic solar cells. *Comptes Rendus Chimie, 9*(5-6), 578-583.

Hara, K., Kurashige, M., Dan-oh, Y., Kasada, C., Shinpo, A., Suga, S.,. & Arakawa, H. (2003). Design of new coumarin dyes having thiophene moieties for highly efficient organic-dye-sensitized solar cells. *New Journal of Chemistry*, *27*(5), 783-785.

In Isoda, H., In Neves M.A., In Kawachi A. and *Alliance for research on North Africa*. (2014).Exploring the seeds and resources for innovation. Sustainable North African society.

In Pandikumar, A. and In Jothilakshmi R. (2014). Potential development in dye sensitized solar cells for renewable energy. *Thermatische Gliederung: Trans Tech Publications.*

In Paranthaman, M.P., In Wong W. and Bhattacharya R. (2016). Semiconductor Materials for solar photovoltaic cells. National Renewable Energy Laboratory, USA.

Imahori, H., Umeyama, T., & Ito, S. (2009). Large π-aromatic molecules as potential sensitizers for highly efficient dye-sensitized solar cells. *Accounts of chemical research*, *42*(11), 1809-1818.

Jason, B. Baxter. (2010). Dye Sensitized Solar Cells: R&D Issues. Department of Chemical and Biological Engineering Drexel University.

Karki, Indra Bahadur, nakarmi Jeevan Jyoti, Mandal Pradip Kumar and Chatterjee Suman. (2012). Dye- Sensitized Solar Cell using extract of Punica Granatun L. pomegranate (Bedana) as a Natural Sensitizer. *Central Department of Physics, Tribhuvan University, Kathmandu,* NEPAL. **2**(12), 81-83**.**

Kroon, J. M., Bakker, N. J., Smit, H. J. P., Liska, P., Thampi, K. R., Wang, P., ... & Würfel, U. (2007). Nanocrystalline dye-sensitized solar cells having maximum performance. *Progress in Photovoltaics: Research and Applications*, *15*(1), 1-18.

Kalyanasundaram, K. (Ed.). (2010). *Dye-sensitized solar cells*. EPFL press.

Kay, A., & Grätzel, M. (1996). Low cost photovoltaic modules based on dye sensitized nanocrystalline titanium dioxide and carbon powder. *Solar Energy Materials and Solar Cells*, *44*(1), 99-117.

Kumara, N. T. R. N., Lim, A., Lim, C. M., Petra, M. I., & Ekanayake, P. (2017). Recent progress and utilization of natural pigments in dye sensitized solar cells: A review. *Renewable and Sustainable Energy Reviews*, *78*, 301-317.

Labouret, A. and Villoz M. (2012). Solar Photovoltaic energy. Stevenage: Institute of Engineering and Technology.

Likhtenshtein G. (2012). Solar Cell Conversion: Hoboken: John Wiley and Sons

Lynn, P.A. (2010). Electricity from Sunlight: An introduction to Photovoltaics. Chichester: Wiley.

Mawyin, J. A. (2009). *Characterization of Anthocyanin Based Dye-Sensitized Organic Solar Cells (DSSC) and Modifications Based on Bio-Inspired Ion Mobility Improvements* (Doctoral dissertation, The Graduate School, Stony Brook University: Stony Brook, NY.).

Marek, P.L. (2013). Biomimetic dye aggregate. Solar cells; springer Science and Business media. Theses Switzerland.

Markart, T. (2000), Solar Electricity. *Chichester; England*: John Wiley and Sons.

McNelis, B. Derrick A. Starr M.R. and UNESCO. (1992). Solar Powered Electricity: A survey of photovoltaic power in the developing Countries. Buorton-on-Dunsmore *Warwickshire, UK: Intermediate Technology Publications in Association with UNESCO.*

Nogi, K. Naito, M. and Yokoyama, T. (2012). Nanoparticle technology handbook. *Amsterdam* Elsevier

Oak Ridge National Laboratory, Industrial Technologies Program (US) and United States. (2012). Photovoltaic Materials. *Washington D.C: Industrial Technologies program.*

O'Regan, B., Grätzel, M., & Fitzmaurice, D. (1991). Optical electrochemistry I: steady-state spectroscopy of conduction-band electrons in a metal oxide semiconductor electrode. *Chemical physics letters*, *183*(1-2), 89-93.

Qifeng Zhang, Guozhong Cao. (2011) Nanostructured Photoelectrodes for dye-sensitized Solar Cells. Science Direct. Washington, *Department of Material Science and Engineering*.

Reddy, P.(2012) Solar Power generation; Technology, new Concepts and Policy. Boca Raton: F L; C R C press.

Sofyan, A. Taya, Taher M. EL-Age Z Hatem S. EL-Ghamri, Monzir S. Abdel-Latif. (2013). Natural Dyes, *international Journal of Material Science and Applications.* **2:**37-42.

Shah, A. V., Schade, H., Vanecek, M., Meier, J., Vallat-Sauvain, E., Wyrsch, N.,. & Bailat, J. (2004). Thin-film silicon solar cell technology. *Progress in photovoltaics: Research and applications*, *12*(2-3), 113-142.

Shakir, S., Abd-ur-Rehman, H. M., Yunus, K., Iwamoto, M., & Periasamy, V. (2018). Fabrication of un-doped and magnesium doped TiO2 films by aerosol assisted chemical vapor deposition for dye sensitized solar cells. *Journal of Alloys and Compounds*, *737*, 740-747.

Salehimarzijarani, B., Dadvar, Z., Mousavi, M., Mirsattari, D., Zali, M. R., & Alizadeh, A. H. M. (2012). Risk factors for post-ERCP cholangitis in patients with pancreatic cancer from a single referral center in Iran. *Asian Pacific Journal of Cancer Prevention*, *13*(4), 1539-1541.

Stubhan, T., Salinas, M., Ebel, A., Krebs, F. C., Hirsch, A., Halik, M., & Brabec, C. J. (2012). Increasing the Fill Factor of Inverted P3HT: PCBM Solar Cells through Surface

Modification of Al-Doped ZnO via Phosphonic Acid-Anchored C60 SAMs. *Advanced Energy Materials, 2*(5), 532-535.

Snaith, H. J., Moule, A. J., Klein, C., Meerholz, K., Friend, R. H., & Grätzel, M. (2007). Efficiency enhancements in solid-state hybrid solar cells via reduced charge recombination and increased light capture. *Nano Letters*, *7*(11), 3372-3376.

Travino, M.R. (2012). Dye-sensitized Solar Cells and Solar Cell Performance Hauppage. New York: Nova Science Publishers.

Wagner, S. Kazmerski L.L. and Coutts T.J. (1986). Copper Indium diselenide for photovoltaic applications *Amsterdam a. o:* Elsevier.

Wang, H., Wei, W., & Hu, Y. H. (2014). NiO as an efficient counter electrode catalyst for dye-sensitized solar cells. *Topics in Catalysis*, *57*(6-9), 607-611.

Wileke, G. and Weber E.R. (2013). Advances in photovoltaic.

Zhao, J. W. (2017). Mechanical Engineering, Material Science and Civil Engineering.

Zollinger, H. (2003) Color Chemistry: Synthesis Properties and applications of organic dyes and Pigments Zurich: *Verlag Helvetica Chemica Acta.*

Zweibel, K. (2013). *Harnessing solar power: The photovoltaics challenge*. Springer.

Zhou, X., Yuping, Z., Zhao, H., Liang, J., Zhang, Y., & Shi, S. (2015). Antioxidant homoisoflavonoidsmmj from Polygonatum odoratum. *Food chemistry*, *186*, 63-68.